Chapter 12
Abdominal Ultrasound—Liver, Spleen and Biliary Tree

James M. Pilcher and Pawan Patel

Keywords Abdominal ultrasound · Scanning technique · Liver parenchyma · Hepatic masses · Biliary obstruction · Splenic masses

12.1 Introduction

Focused abdominal ultrasound in critically unwell patients, can provide valuable diagnostic information regarding specific pathologies of the abdominal viscera or peritoneal cavity; evaluate blood flow within the main arteries and veins of the abdomen and be used to guide intervention procedures, such as percutaneous drainages [1]. The technique differs to that practised in radiology departments, where traditionally a comprehensive survey of the whole abdomen and pelvis is performed, instead targeting individual organs or quadrants of the abdomen, to answer specific clinical questions. In addition abdominal ultrasound in the acutely ill has its own challenges, with oedematous tissues, excessive bowel gas or free air in the post-operative patient, external monitoring devices, open wounds, limited patient positioning and ability to breath hold; all compromising either image quality or access to adequate views. In this chapter an approach to abdominal ultrasound in acutely unwell patients, followed by a description of ultrasound findings in a selection of pathologies affecting the liver, biliary system, spleen, bowel and peritoneum. The pathologies chosen are those that the author believes not infrequently arise as clinical queries and that can often be answered with the careful use of targeted ultrasound.

J. M. Pilcher (✉)
Consultant Radiologist, St George's University Hospitals NHS Foundation Trust, Blackshaw Road, Tooting, London SW170QT, UK
e-mail: James.Pilcher@stgeorges.nhs.uk

P. Patel
Locum Consultant, St George's University Hospitals NHS Foundation Trust, Blackshaw Road, Tooting, London SW170QT, UK

A. Walden et al. (eds.), *Ultrasound in the Critically Ill*,
https://doi.org/10.1007/978-3-030-71742-1_12

12.2 Artefacts

When scanning the upper quadrants of the abdomen, the operator should be aware of potential artefacts generated by air-tissue and fluid-tissue interfaces. The mirror image artefact can potentially be generated at any air-tissue interface, which in the upper quadrants is typically the interface between either the liver or spleen and the pleura-aerated lung interface against the diaphragm. The artefact generates a faint image of the liver or splenic architecture on the cranial side of the diaphragm i.e. within the aerated lung (Fig. 12.1). This artefact will be lost in the presence of a pleural effusion, which itself can be a helpful diagnostic finding. If the is a small amount of fluid partially surrounding the liver or spleen, at certain scanning angles a diffraction artefact can be generated, giving the impression of a defect/step in the adjacent hemi-diaphragm (Fig. 12.2) [2]: this is a particular potential pitfall when scanning trauma patients.

Some of the artefacts encountered in the abdomen can be helpful by increasing diagnostic confidence. Acoustic shadowing is the loss of sonographic information beyond an interface or structure that is either strongly reflective or absorptive of ultrasound. Within the gallbladder, gallstones will generally generate this artefact, seen as a well-defined black/dark-grey line radiating down beyond the gallstone (Fig. 12.3). Likewise renal stones, if large enough, will also generate this artefact. Unfortunately gas within the bowel will do the same, preventing visualisation of deeper structures: although the nature of the shadowing is different, being less defined and more mixed in its reflectivity (dirty shadowing). Acoustic enhancement occurs beyond structures that allow more sound through than the adjacent tissue interfaces, resulting in an increase in the brightness of the tissue beyond. Structures that are very uniform in their acoustic properties, or are low in density will typically

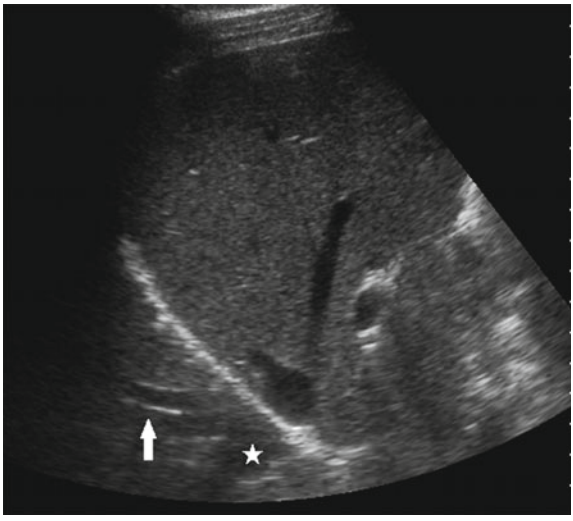

Fig. 12.1 Longitudinal oblique view of the right lobe of the liver and hemidiaphragm, the latter is seen as a curvilinear echogenic interface. The hepatic veins (arrow) and IVC (star) are seen cranial to the hemidiaphragm due to mirror artefact

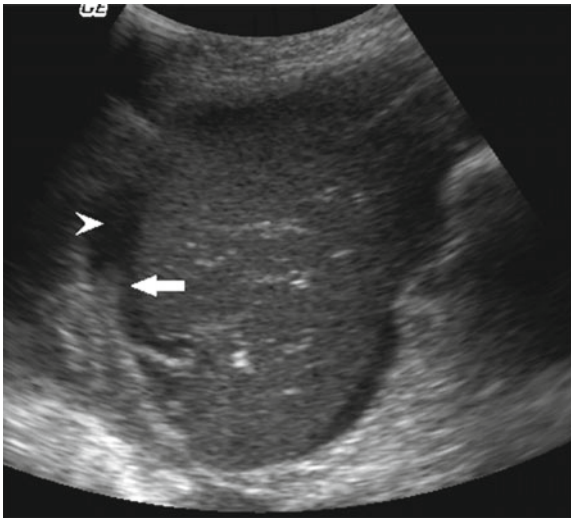

Fig. 12.2 Longitudinal oblique view of the spleen and left hemidiapharagm. There is a small volume of free fluid partially surrounding the spleen (arrowhead), which causes a diffraction artefact between the spleen and the left hemidiaphragm, making the latter appear fractured (arrow)

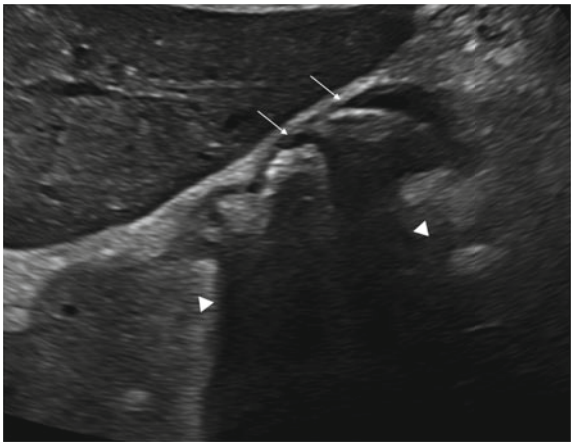

Fig. 12.3 Longitudinal oblique view through the gallbladder containing multiple echogenic gallstones (arrows). These are causing acoustic shadowing (arrowheads), with loss of tissue information beyond the gallstones

do this: such as a cyst in the liver (Fig. 12.4), or a solid mass with very uniform cell content within it such as lymphoma. Reverberation artefact occurs where the returning echo from a strongly reflecting surface, reflects back and forth between that interface and another strongly reflecting surface (usually the skin surface-probe interface) to produce equally spaced linear echoes that weaken over depth. Intensivists are very familiar with this artefact in lung ultrasound and likewise in the abdomen this can be seen distal to a straight, continuous air interface in the bowel, or when there is free air adjacent to the anterior peritoneum.

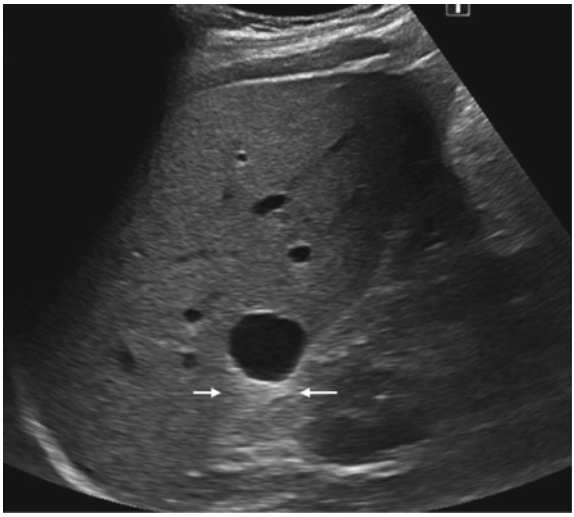

Fig. 12.4 A simple cyst in the liver demonstrates increased parenchymal reflectivity beyond the posterior wall of the cyst (arrows), known as acoustic enhancement

12.3 Scanning Technique

The vast majority of abdominal ultrasound examinations carried out on the intensive care unit can be performed to a satisfactory diagnostic standard using a standard curvilinear array, operating in a frequency range of between 2 and 6 MHz. Occasionally it is useful to have the option of a higher frequency linear array, such as the vascular access probe, to perform targeted assessment of the liver surface, bowel loops, and peritoneum. The abdominal preset should be selected and the operating frequency of the probe optimised for the patient being scanned: the lower frequency option being selected for the more challenging patient. On modern machines this is often labelled as either: resolution, general, penetration setting; or easy, medium and difficult. There is also usually the option of turning on or off harmonic imaging, which can improve tissue contrast and reduce clutter in the image. Further adjustments to the grey scale image can be made by adjusting the extent of compound imaging used in generating the image, improving edge definition, but also smoothing the image (Fig. 12.5). The depth should be adjusted to display the entire organ under investigation and as a general starting point setting the depth to 15 cm should allow adequate visualisation of most of targeted organs described in this chapter. If the focal zone can be adjusted, this needs to be set at the level of diagnostic interest and therefore may require repeat adjustment during the examination. If colour Doppler is being used the assess flow in the hepatic vessels, the colour box should be adjusted to only cover the area of interest and thought given to optimising the scale setting and gain control.

Although the intensivist will frequently perform a targeted approach to abdominal ultrasound in order to answer a specific question about one organ, the following description outlines a more general approach to the upper abdominal

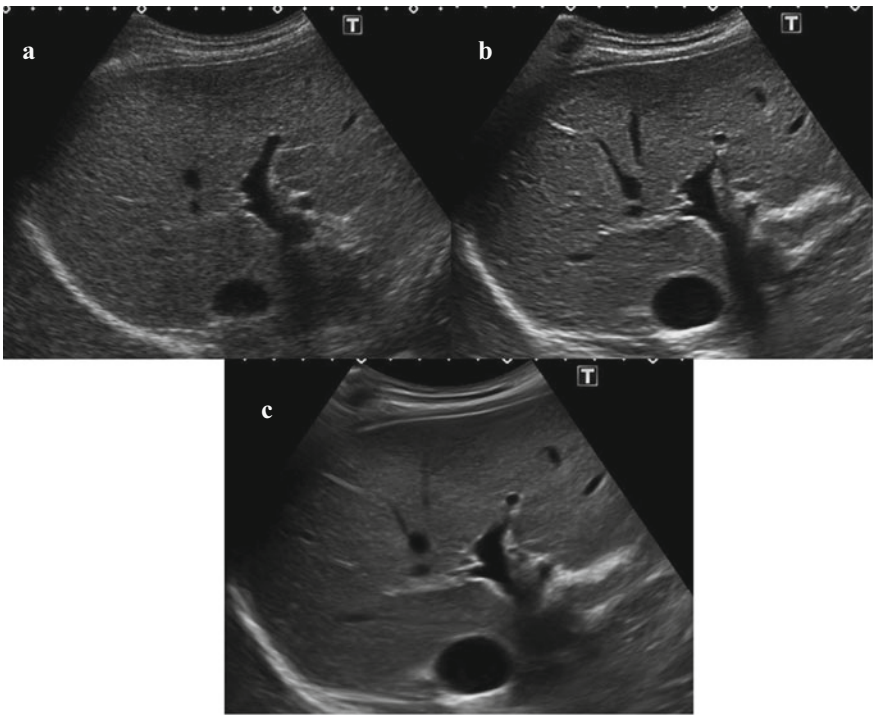

Fig. 12.5 Three identical views through the right lobe of the liver, with increasing image compounding (**a**, **b**, **c**). This progressively reduces the speckle (graininess) in the liver parenchyma and increases vessel wall definition

organs in an attempt to highlight their spatial relationship on ultrasound. The initial scan is performed with the patient in the supine position. The abdominal probe is placed transversely in the midline, just below the xiphisternum, with the side marker on the probe orientated towards the right side of the patient. By rocking the probe in an up and down motion, angled sweeps through the left lobe of the liver can be obtained without having to move the probe across the skin surface (Fig. 12.6): This sweeping approach will also usually cover the base of the heart, gastro-oesophageal junction, proximal aorta with its mesenteric branches, and part of the pancreas. The probe is then slid laterally to sit directly below the right costal margin and the same rocking action repeated to image the right lobe of the liver. This is repeated, sequentially repositioning the probe more laterally, until the whole of the right lobe of the liver has been covered. If the patient is able to breath-hold, then the image quality can be enhanced by performing these scan sweeps in suspended deep inspiration. If this is not possible, then further views of the liver can be obtained by placing the probe into one of the lower rib spaces, although the angled

sweep is then limited by acoustic shadowing from the ribs. The liver is then scanned in longitudinal section, by either sliding and rocking the probe along below the costal margin, preferably with the patient in arrested inspiration; or if the subcostal approach is limited, by scanning across the lower ribs while altering the angle of the probe to compensate for the rib shadows. Views of the far right lateral edge of the liver can also be obtained by placing the probe in the subcostal midclavicular line and angling the probe face towards the right shoulder to catch the posterior superior region of the right lobe (Fig. 12.6). Rolling the patient onto their left side, may also improve views of the lateral aspect of the liver, with the probe placed longitudinally along the anterior axillary line (subcostal or intercostal) and angled posteriorly. This latter approach is can also be used for gaining a longitudinal image of the gallbladder, although this is usually demonstrated just as well when the patient is supine, with the probe placed in an identical location. Transverse views of the gallbladder are obtained, using probe positioning as for transverse views of the right lobe of the liver. The porta hepatis can usually be seen with a longitudinal oblique approach similar to that for the gallbladder, but with the probe orientated less posteriorly. The common bile duct (CBD) can sometimes be seen well enough with this approach, but if not the patient is then rolled onto their left side and the probe placed directly over the line of the CBD in a midclavicular subcostal location, with the probe rotated slightly clockwise off the transverse (Fig. 12.6). A longitudinal positioning of the probe, just to the right of the midline can sometimes demonstrate the distal CBD as it passes through the head of the pancreas (Fig. 12.6). Going back to the starting position and moving to the left, identical positioning of the probe along the left costal margin and lower rib spaces, will afford views of the stomach, tail of pancreas and most of the spleen. A good longitudinal view of the spleen can be obtained, by placing the probe between the mid and posterior axillary line and rotating the probe obliquely so that it lies in one of the lower rib spaces: Sometimes this is easier to perform with the patient rolled slightly onto their left side, again rocking the probe to sweep through the spleen from anterior to posterior. Rotating the probe 90° in this location will enable transverse sweeps of the spleen, while sliding the probe caudally from this position will bring the left kidney into view. Because of the more posterior location of the spleen, breath holding is often unhelpful in improving its visualisation on ultrasound, as the lower lobe of the left lung extends down around it casting an acoustic shadow.

By adopting the above approach it is usually possible to fully assess the liver, gallbladder, biliary tree, stomach and spleen, with other abdominal structures captured during the sweeping motion at each probe position. For ultrasound of the bowel a more targeted approach is required and this is outlined in the section in the subsequent chapter on bowel. Likewise for the detection of intraperitoneal free fluid a more focused approach can be used, which includes the pelvis and this is also described in the subsequent chapter.

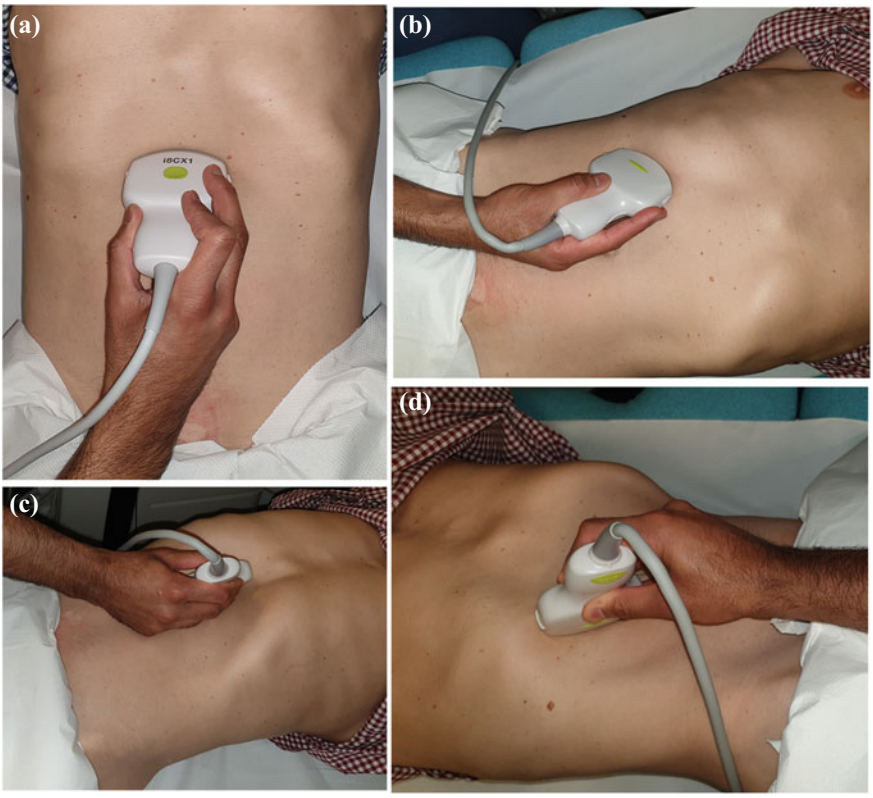

Fig. 12.6 Abdominal probe positions for: **a** Transverse sweep through the left lobe of the liver; **b** Additional views of the posterior superior right lobe of liver; **c** Longitudinal view along the common bile duct, with patient in the left lateral decubitus position; **d** Longitudinal view through the head of the pancreas to demonstrate the distal CBD

12.4 Liver

Ultrasound is the first line imaging technique for the liver on the intensive care unit, whether in the evaluation of the jaundiced patient, looking for a source of sepsis, confirming portal vein patency or assessing suspected hepatic venous congestion.

12.4.1 Anatomy

The liver lies in the right upper quadrant, and is made up of three lobes: the right and left lobe separated by the main lobar fissure, and the caudate lobe. The right and left lobes are further subdivided into anterior and posterior segments, and medial

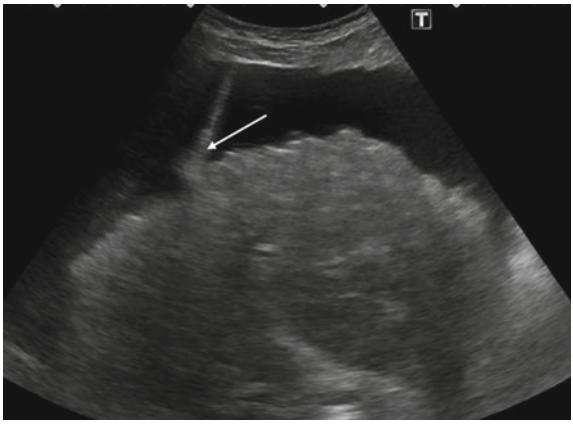

Fig. 12.7 Transverse scan through a cirrhotic liver, in a patient with abdominal ascites. The ligamentum teres and falciform ligament are seen as an echogenic triangle arising off the liver surface to reach the anterior abdominal wall (arrow)

and lateral segments respectively. It has a domed smooth superior surface, in contact with the right hemi-diaphragm and adjacent ribs, and a more contoured inferior or visceral surface that is orientated to face postero-medially. The liver is surrounded by Glisson's capsule, which on high resolution ultrasound can be appreciated as a thin linear echo along the liver surface. Adherent peritoneum then overlies most of the liver, except for the bare area posteriorly, which is bordered by folds in the peritoneum, namely the right and left triangular ligaments and the coronary ligament, which divide the subphrenic and subhepatic peritoneal spaces. Although these ligaments are not seen at ultrasound, anteriorly the falciform ligament and ligamentum teres can be seen in the presence of ascites, as an echogenic triangular structure arising off the anterior surface of the liver and extending down to the umbilicus (Fig. 12.7). The ligamentum teres contains tiny veins, normally invisible at ultrasound, but these dilate in patients with portal hypertension and can then be identified with colour Doppler, shunting portal venous blood to the umbilicus (Fig. 12.8).

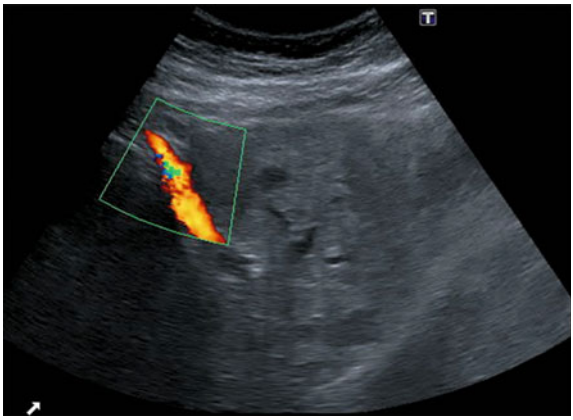

Fig. 12.8 Transverse view through the left lobe of the liver with colour Doppler showing large collateral vein exiting the liver in the ligamentum teres towards the umbilicus

Vascular input to the liver is from the portal vein (approximately 75% of inflow) and the hepatic artery (25%).These enter the liver at the porta hepatis, with the portal vein positioned posterior to the hepatic artery and the adjacent common hepatic duct. Positioning the abdominal probe in an oblique orientation along the right anterior axillary line can demonstrate this vascular anatomy nicely and enable Doppler assessment of the main portal vein (Fig. 12.9). On this view the portal vein is relatively straight, while the hepatic artery is more tortuous and may not be seen in its entirety. Just before entering the porta the hepatic artery divides into right and left branches, with the right hepatic artery passing between the portal vein and common hepatic duct to enter the liver: although there are a number of anatomical variations recognised. Within the liver the portal vein divides into right and left branches, with the right passing transversely through the liver for a short length before dividing into anterior and posterior branches, while the left branch curves anteriorly through the left lobe of the liver to divide into segmental branches. The intrahepatic portal veins have echogenic walls on ultrasound due to their fibromuscular walls, while the accompanying hepatic artery and bile duct increases the number of adjacent reflective interfaces. Three main hepatic veins drain the liver: the left runs between the medial and lateral segments of the left lobe of the liver, the middle hepatic vein lies in the sagittal plane between the right and left lobes of the liver and the right runs in a coronal plane between the anterior and posterior segments of the right liver. The left and middle hepatic veins usually join together before draining into the IVC. Due to their orientation and thin walls the hepatic veins usually appear as echolucent tubular structures on ultrasound (Fig. 12.10), with no wall interface, this appearance and their orientation within the liver enables their distinction from portal veins at ultrasound.

As already alluded to, the lobes of the liver are divided into segments using a classification originally described by a French surgeon Claude Couinaud [3]. A detailed description of this classification is beyond the scope of this text, but both the right and left lobes of the liver contain four segments; each with a central

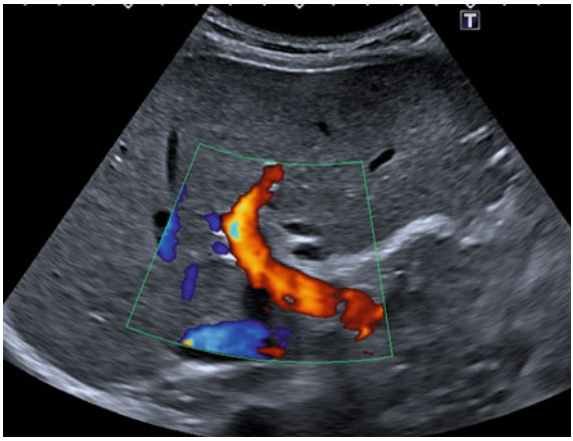

Fig. 12.9 Longitudinal oblique view through the main portal vein with colour Doppler confirming flow towards the liver i.e. coded red

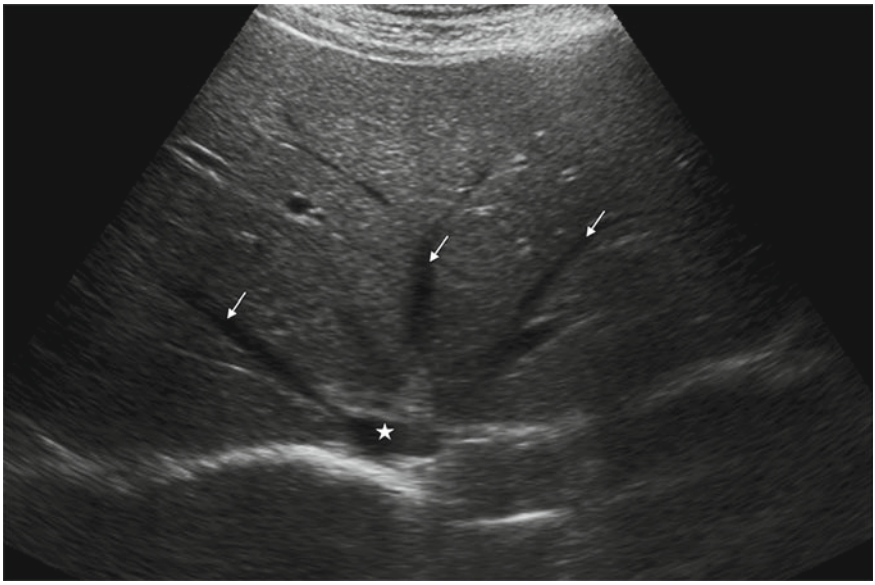

Fig. 12.10 Right subcostal transverse view through the liver showing the hepatic veins (arrowed) confluence with the IVC (star)

feeding portal vein, with adjacent segments margined by one of the hepatic veins (Fig. 12.11). The segments are numbered I–VIII, with segment I representing the caudate lobe, this lies posterior to the rest of the left lobe of the liver, which contains segments II–IV. The right lobe contains segments V–VIII, with V and VIII

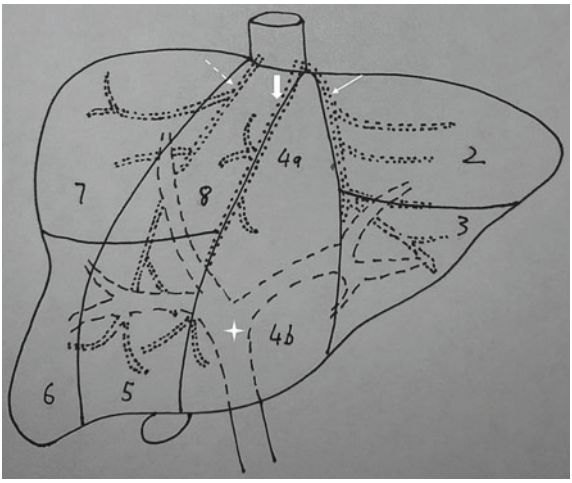

Fig. 12.11 The Couinaud classification divides the liver into eight segments, each of which has its own blood supply and biliary drainage. The centre of each segment contains the portal triad, consisting of a branch of the hepatic artery, portal vein and a bile duct. Venous drainage is at the periphery of the segments from hepatic vein branches. The middle hepatic vein (thick arrow) divides the liver into the right and left lobes. The left hepatic vein (thin arrow) divides the left lobe into a medial (segment 4a and b) and lateral part (segment 2 and 3). The right hepatic vein (dashed arrow) divides the right lobe into anterior (segment 8 and 5) and posterior (segments 7 and 6) parts. The portal vein (star) divides the liver into superior and inferior segments. The caudate lobe is segment 1

Table 12.1 Dimensions of normal liver at abdominal ultrasound [4]

Diameter	Mean ± SD (cm)
Midclavicular Longitudinal	10.5 ± 1.5
Midclavicular anteroposterior	8.1 ± 1.9
Midline Longitudinal	8.3 ± 1.7
Midline anteroposterior	5.7 ± 1.5

positioned anterior to VII and VI. When scanning the liver, the right and left lobes can be targeted individually, allowing the segmental anatomy to be appreciated as described in the section on scanning technique.

12.4.2 Liver Size

Wide variation in the configuration of the liver makes overall assessment of liver size difficult. There are defined linear values, based upon measurements taken from 1000 healthy volunteers [4], enabling some assessment of right and left lobe size measured at the midclavicular line and midline respectively; this can be useful in certain situations, such as assessing chronic liver disease (Table 12.1). Comparing the relative size of the caudate lobe to the right and left lobe is also useful in this situation as the caudate may enlarge in cirrhosis or hepatic vein occlusion. Normally when scanning in the transvers plane, at the level of the porta, the diameter of the caudate should be less than two-thirds the diameter of the right lobe; while the anteroposterior distance of the caudate should be less than half that of the left lobe.

12.4.3 Normal Liver Parenchyma

It is important for the operator to be comfortable with how normal hepatic echotexture appears on their ultrasound system (it will differ slightly between ultrasound units), in order to detect parenchymal changes that may indicate disease. This may be due to underlying chronic inflammation, deposition disorders, end stage fibrotic disease or a reflection of altered metabolism. The main two patterns to recognise however are fatty change and cirrhosis.

Normal liver echotexture consists of fine interleaving echoes, producing a fairly consistent speckle pattern from the front to the back of the liver. However this pattern can be altered by the operator changing the scanning frequency, turning on/off harmonic imaging or altering the spatial compounding level and the operator should be comfortable with the impact these adjustments may have on the final image (Fig. 12.5). Normal liver reflectivity is described as similar or slightly brighter than that of the adjacent right kidney, providing the latter is normal, and therefore possibly a more reliable comparison is the spleen, which is typically slightly more echogenic than the liver. Within the liver, the portal tracts are usually quite reflective, seen as bright lines outlining the portal veins, while the hepatic veins usually have no reflective wall, unless they are scanned in a perpendicular orientation, with respect to the ultrasound probe.

12.4.4 Abnormal Liver Parenchyma

Fatty liver is one of the commonest abnormalities found on abdominal ultrasound, with many associations (Table 12.2), and is due to increased levels of triglycerides within the hepatocytes. It results in a diffuse increase in parenchymal reflectivity, the liver becoming more echogenic than the adjacent kidney and spleen, although the texture remains fine and uniform. In some cases however areas of focal fatty sparing can occur, typically around the gallbladder, next to the ligamentum teres and at the bifurcation of the main portal vein. These cause focal areas of relatively reduced reflectivity in the liver with rather geometric shapes, typically having straight edges (Fig. 12.12). Colour Doppler can be used to confirm normal anatomy of hepatic vessels passing through these areas of reduced reflectivity. Occasionally fatty change can take on a more rounded appearance within the liver and then closer interrogation is required, including the use of contrast enhanced imaging, to exclude an underlying mass lesion.

Diffuse fatty change is usually described as mild, moderate or severe; mild showing a slight increase in liver reflectivity, moderate when there is loss of hepatic vessel wall definition, with poor visualisation of the posterior liver and severe when there is very limited visualisation of the hepatic vessels, posterior liver and hemidiaphragm [5] (Fig. 12.13). Sometimes fatty change is more focal in the liver, when its shape and location is similar to that described above for focal fatty sparing, although these locations now appear brighter than the adjacent liver parenchyma. Again, as with focal sparing, normal hepatic vessels can be shown to pass through these areas on colour Doppler.

Cirrhotic patients carry significant co-morbidities and therefore it is important to be able to recognise these parenchymal changes in patients who are as yet undiagnosed. The cirrhotic liver can take on a number of appearances, depending upon it aetiology, presence of portal hypertension and associated malignancies. Typically

Table 12.2 Conditions associated with fatty liver

Common	Rare	Congenital
Alcohol	Pregnancy	Organic aciduria
NAFLD	Starvation	Aminoacidopathy
Obesity	Rapid weight loss	Glycogen storage disorders
Hyperlipidaemia	Total parenteral	α1—antitrypsin deficiency
Hepatitis B and C	nutrition Jejunal-ileal bypass Radiotherapy	Wilson's disease Haemochromatosis Cystic fibrosis
Drugs		
Steroids Chemotherapy		
Amiodarone Valproic acid		

NAFLD = Non-alcoholic fatty liver disease

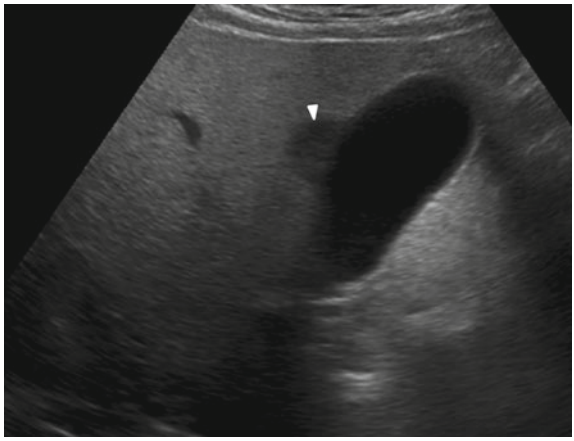

Fig. 12.12 Longitudinal oblique view through segment 5 of the liver shows a well-defined area of relatively reduced reflectivity, with respect to the background liver, adjacent to the gallbladder. The shape and location is typical for focal fatty sparing (arrowhead). The background liver shows diffuse increased reflectivity indicating steatosis

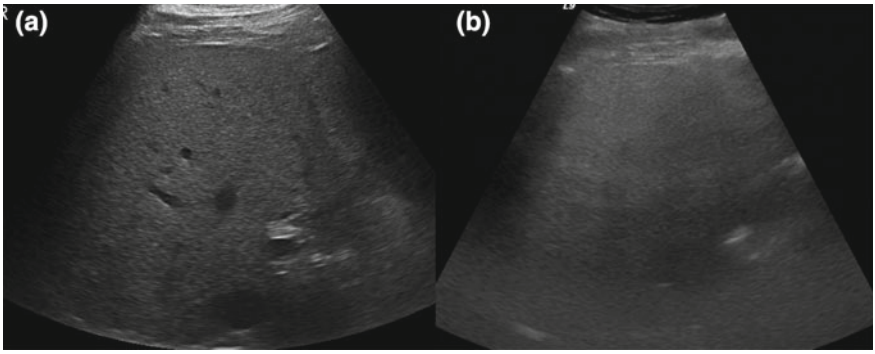

Fig. 12.13 Diffuse fatty liver: **a** Moderate fatty liver, with loss of vessel wall definition in the periphery of the liver and some loss of parenchymal detail towards the back of the liver. **b** Severe fatty change, with marked attenuation and almost no appreciation of hepatic vessels

there is a "coarsening" of the parenchymal liver texture due to focal regenerating nodules and surrounding fibrosis. Careful scrutiny of the liver surface shows an irregular contour due to focal nodules: which are seen more clearly in the presence of ascites (Fig. 12.14). If available, a more detailed evaluation of the liver surface contour can be made by switching to a higher frequency linear array probe (Fig. 12.15). There is often a reduction in size of the right lobe of the liver, with relative enlargement of the caudate lobe and with the onset of portal hypertension the portal vein becomes dilated (> 13 mm). If spectral Doppler interrogation is

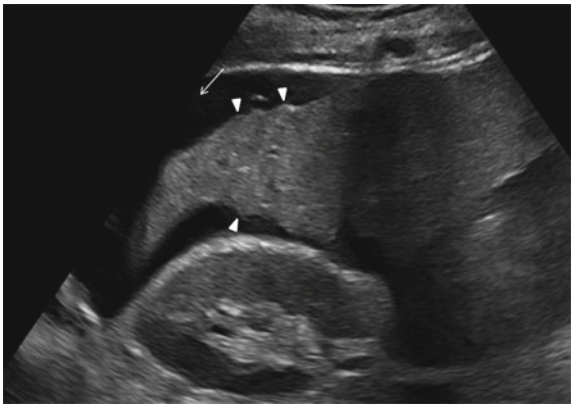

Fig. 12.14 Transverse view of a cirrhotic liver, with surrounding ascites (arrows) and underlying right kidney. The liver surface demonstrates a nodular contour in keeping with cirrhosis (arrowhead)

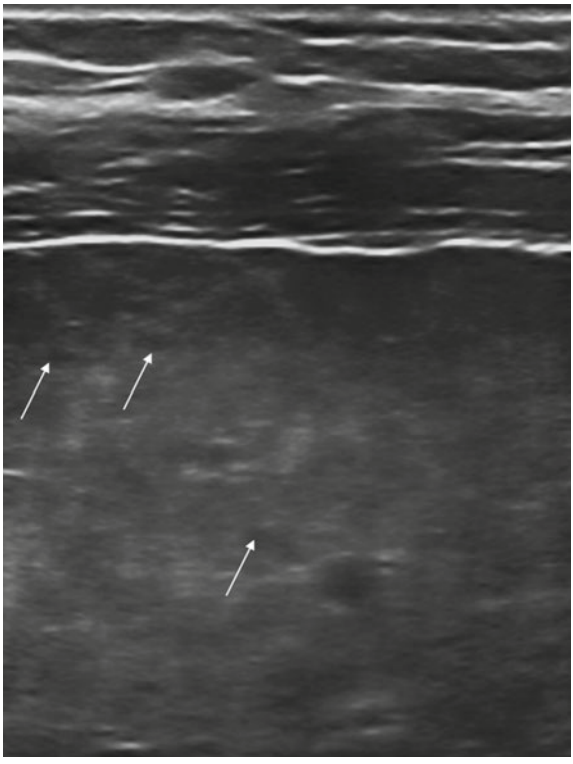

Fig. 12.15 Higher frequency linear array scan through liver that initially looked mildly heterogeneous on a curvilinear array. This confirms multiple low reflective nodules (arrows), surrounded by echogenic reticular pattern of fibrosis, consistent with cirrhosis

applied to the portal vein, an angle corrected peak portal vein velocity of <15 cm/s is consistent with portal hypertension (Fig. 12.16). Colour Doppler can be used to identify collateral vessels around the left lobe of the liver, small bowel mesentery and at the splenic hilum, where there may also be splenomegaly.

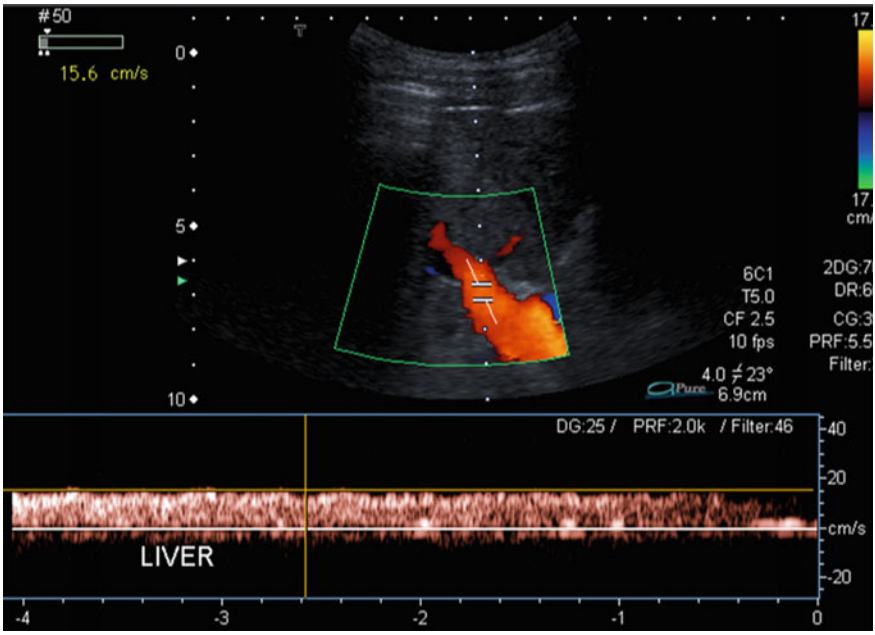

Fig. 12.16 Angel corrected spectral Doppler trace through the main portal vein, in a patient with cirrhosis, demonstrating a reduced peak portal vein velocity of 15.6 cm/s. The main portal vein is also dilated

12.4.5 Inflammatory Conditions

Inflammatory/infective conditions of the liver tend to be either diffuse or focal and ultrasound has an important role to play in both the initial identification of these and sometimes their management.

The inflammatory liver is a well-recognised, but non-specific pattern change seen in liver parenchymal echotexture and is likely to be a finding in a number of intensive care patients. Also known as the "starry sky" appearance, this represents an increase in periportal tract reflectivity, sometimes associated with a thickening of the bright interfaces outlining the portal veins. The background liver parenchyma is perceived as being darker than its usual mid-grey reflectivity (Fig. 12.17), and depending upon the underlying cause, the liver may also be slightly enlarged. Although these findings are often attributed to a diagnosis of viral hepatitis, when there is also typically gallbladder wall thickening [6], this has a broad differential diagnosis, including a normal variant in slim individuals (Table 12.3).

Pyogenic liver abscesses may result from direct extension of an infective process in the biliary tree, portal venous dissemination from an abdominal source, or haematogenous spread from a distant infection. On ultrasound pyogenic liver abscesses are highly variable in their appearance: sometimes resembling a simple

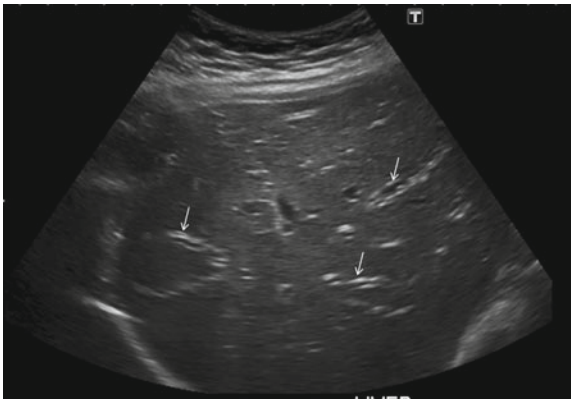

Fig. 12.17 Transverse view of the liver, showing increased reflectivity of the periportal tracts right out to the periphery of the liver (arrows)

Table 12.3 Differential for increased periportal reflectivity at liver ultrasound

Diagnosis	Additional findings
Acute viral hepatitis Infectious mononucleosis	Thick walled gallbladder Splenomegaly and lymphadenopathy
Toxic shock syndrome	
Congestive cardiac failure	Hepatic vein enlargement ± ascites
Periportal fibrosis Cholangitis	Coarsened liver parenchyma Thick walled common bile duct
Inflammatory bowel disease	Bowel wall thickening and hyperaemia
Schistosomiasis	
Burkitt'slymphoma	
Normals	

anechoic cyst to a solid echogenic mass, or multiple partially cystic nodules suggestive of metastatic disease. Early abscess formation often appears solid on ultrasound, but frequently demonstrates slightly reduced reflectivity and posterior acoustic enhancement, suggesting a more cystic content (Fig. 12.18). With progressive necrosis they become more heterogeneous in echotexture, with central cystic change containing debris, echogenic septations and if it is a gas forming organism, highly reflective foci showing reverberation artefact or shadowing [7]. Certain pathogens (e.g. Klebsiella Pneumoniae) however can result in a deceptively solid appearing lesion, with no through transmission of sound [8], although circumferential increased vascularity on colour/power Doppler may suggest an inflammatory process.

The sensitivity of ultrasound for detection of liver abscess is up to 97% [9], but the variable ultrasound appearances can overlap with those seen in haemorrhagic liver cysts, focal haematoma and malignant tumours. Where there is diagnostic uncertainty, further imaging with CT or MRI may be required, or if there is the relevant experience a contrast enhanced ultrasound (CEUS) study reveals a fairly

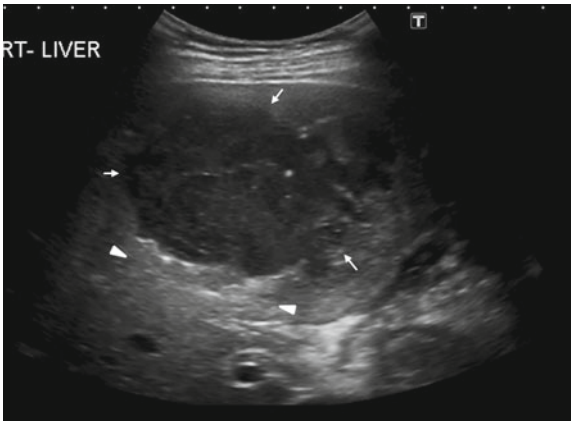

Fig. 12.18 Early liver abscess (arrows), with a mainly solid appearance, but through transmission of sound indicating this may be party liquefied (arrowheads). No internal vascularity was seen on subsequent Doppler interrogation

characteristic enhancement pattern in the region of the liver abscess [10]. Once confirmed, ultrasound can be used to guide either needle aspiration of the abscess or insertion of a pigtail drainage catheter. Although both of these techniques can expedite resolution of the abscess, a greater reduction in abscess volume can be achieved with single pigtail drainage [11] using ultrasound monitoring to ensure the drain remains correctly sited. If heavily loculated, or multi-focal in nature, attempts at percutaneous drainage may only produce a few millilitres of abscess content.

12.4.6 Focal Hepatic Masses

Focal liver lesions are not infrequently seen when assessing the liver with ultrasound and familiarity with some of the more common lesions and when to ask for further imaging is important for the operator. When assessing focal liver lesions, as for mass lesions elsewhere in the abdomen, the operator should determine: it's location in the liver, the relative reflectivity of the lesion with respect to the background visceral parenchyma; it's uniformity of texture; shape and margins; whether it is solitary or multifocal; look for any associated artefacts e.g. acoustic shadowing and use colour/power Doppler to determine whether it has increased or reduced vascularity. Some focal liver lesions can be confidently diagnosed with standard ultrasound alone, but many have features that overlap between benign and malignant. These will require further evaluation with CEUS, CT or MRI.

12.5 Haemangiomas

Cavernous haemangiomas are the commonest benign mass lesion in the liver with a prevalence of 0.5–20%. These can be multifocal in 10–50% of cases [12], more commonly seen in the right lobe and towards the periphery of the liver. The multiple interfaces generated by a combination of blood spaces and fibrous septae results in a relatively uniform echogenic, rounded, lobular mass, typically <3 cm in size (Fig. 12.19). This may show some posterior through transmission of sound on grey scale imaging, but due to the sluggish flow of blood within it, rarely demonstrates any flow on colour/power Doppler. If the ultrasound appearances are typical then no further imaging is required; however as they get larger, central areas of haemorrhage, necrosis and fibrosis, can result in a more heterogeneous pattern of reduced central reflectivity, although often maintaining their echogenic margin. These changes make confident diagnosis with ultrasound more challenging and will require either CEUS or MRI with contrast to confirm the typical enhancement pattern seen with haemangiomas. If very large, as with other benign liver masses, haemangiomas can cause symptoms through compression of the biliary tree, inferior vena cava, portal vein or adjacent viscera; all of which can potentially be demonstrated at ultrasound.

12.5.1 Hepatic Cyst

Seen in 2–4% of the population, simple hepatic cysts have a classical appearance on ultrasound of a rounded, anechoic structure, with an imperceptible wall and posterior acoustic enhancement. A single thin septation may be seen, but thick septations or echogenic mural nodules raise the possibility of a cystic mucinous tumour and require further evaluation with CEUS or contrast enhanced CT/MRI.

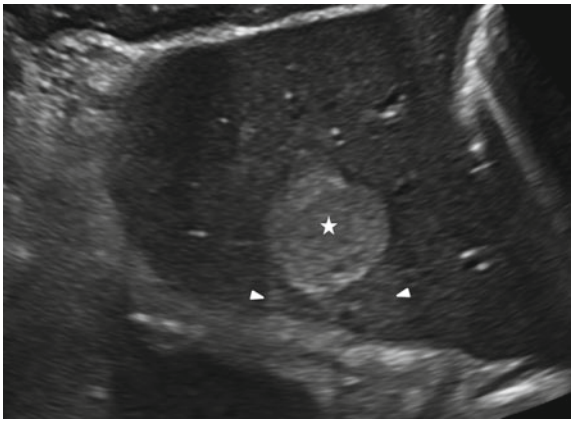

Fig. 12.19 Well defined, lobular, uniformly echogenic focal liver lesion (star), with posterior acoustic enhancement (arrowheads) in keeping with a hepatic haemangioma

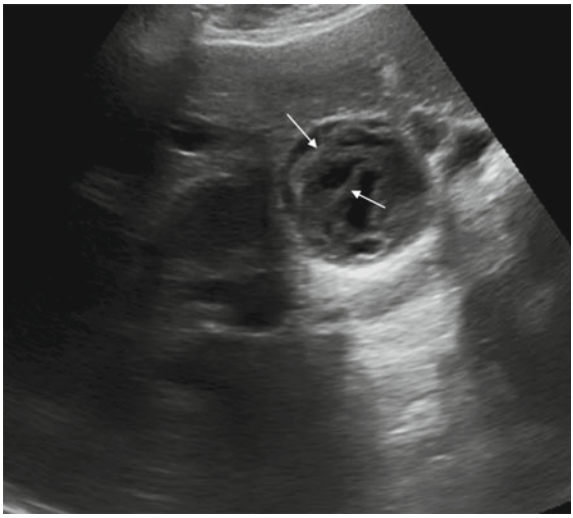

Fig. 12.20 Transverse view through left lobe of the liver showing a haemorrhagic cyst, with thick septations (arrows) and through transmission of sound, deep to the cyst. This will require further characterisation with contrast imaging (ultrasound, CT, MRI) to confirm there is no blood flow in the septations

Haemorrhagic change can also cause thickened septations, internal echoes and wall thickening, which requires further evaluation to confirm lack of enhancement in the septations (Fig. 12.20). Other complications of hepatic cysts are rupture and infection, both of which are rare in patients with only one or two cysts, but in patients with polycystic liver disease these complications become more common.

Polycystic liver disease is an autosomal dominant condition, sometimes associated with autosomal dominant adult polycystic kidney disease, resulting in multiple hepatic cysts throughout the liver (Fig. 12.21). Due to the sheer number of cysts, the complications already described are more likely to occur along with

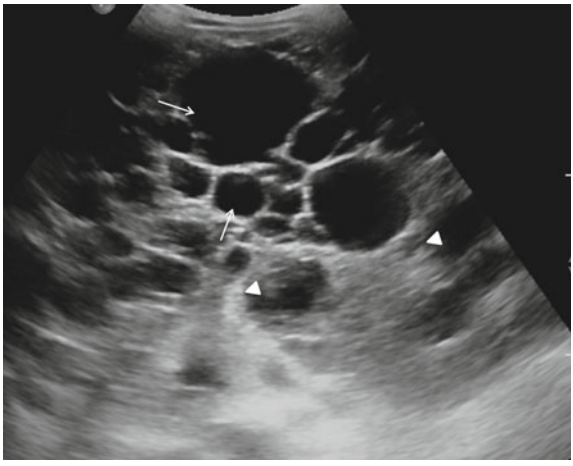

Fig. 12.21 Polycystic liver disease. The liver parenchyma is almost completely replaced by innumerable, well circumscribed, anechoic cysts (arrows). There are regions of posterior acoustic enhancement, in keeping with features of fluid content (arrowheads)

extrinsic compression of adjacent structures, namely the IVC, portal vein, biliary system and adjacent stomach.

12.5.2 Malignant Focal Liver Lesions

Liver metastases are the most common malignant liver lesion by a significant percentage, with the two most common primary tumours being hepatocellular carcinoma and cholangiocarcinoma. Liver metastases are typically multifocal, discrete lesions detected incidentally as they are usually asymptomatic. They are variable in their sonographic appearance, ranging from hypoechoic to hyperechoic or a mixed reflectivity; the classic pattern of the latter is of an echogenic centre, with hypoechoic margin (Fig. 12.22), also referred to as target lesions. Most metastases will show little if any vascularity on colour or power Doppler and assessment of vascularity in these lesions requires the addition of microbubble contrast or alternative cross-sectional imaging. Rarely extensive metastatic infiltration of the liver can present with obstructive jaundice due to intrahepatic compression of numerous biliary radicals. Hepatocellular carcinoma may present acutely with spontaneous rupture and subsequent haemoperitoneum, or portal vein thrombosis as a result of portal vein invasion. Both of these complications can be diagnosed at ultrasound (see later text). As with liver metastases, hepatocellular carcinoma is variable in its sonographic appearance, tending to be hypoechoic when small, with a more mixed, increased reflective pattern centrally as it grows in size [13]. The additional findings of satellite nodules, thrombosed adjacent veins and

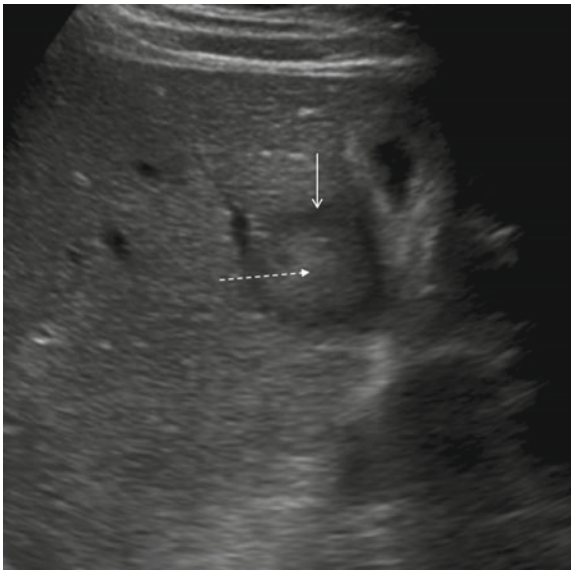

Fig. 12.22 "Target lesion": Focal liver lesion with an echogenic centre (dashed line) and hypoechoic peripheral rim (arrow). This appearance is strongly suggestive of a liver metastasis

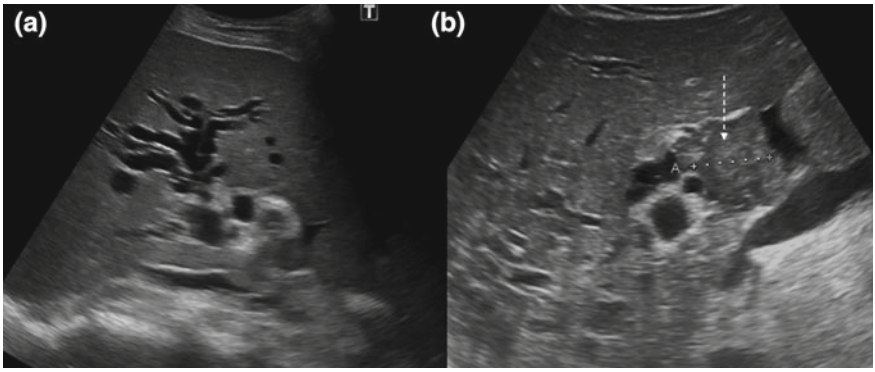

Fig. 12.23 **a** Transverse image through right lobe of liver showing numerous branching tubular structures (too many), in keeping with intrahepatic bile duct dilatation. **b** This is seen to be secondary to an obstructing lobulated mass at porta hepatis (dashed arrow)

detectable vascularity on colour/power Doppler also support a likely diagnosis of hepatocellular carcinoma, particularly in the presence of background cirrhosis. Intrahepatic cholangiocarcinomas are classified as either periductal -infiltrating or intraductal-mass forming and most commonly arise at the bifurcation of the hepatic ducts, resulting in intrahepatic duct dilatation in both lobes of the liver, obstructive jaundice and episodes of cholangitis. Sonographically the dilated intrahepatic bile ducts produce a crab-like pattern within the liver on transverse scanning, with the dilated bile ducts seen as black tubular structures radiating out from the porta (Fig. 12.23). The actual tumour itself can be difficult to appreciate on ultrasound, particularly the periductal type, often being relatively isoechoic to adjacent liver parenchyma, with the abrupt cut-off of the dilated intrahepatic bile ducts the only clue to the cause. Larger or intraductal tumours are more apparent on ultrasound and are of variable reflectivity. More peripherally located, lobar intrahepatic tumours tend to be clinically silent and at ultrasound there may be regional atrophy of the liver parenchyma, with crowding of the dilated bile ducts, adjacent portal veins and hepatic artery (Fig. 12.24). As with liver metastases, ultrasound suspected hepatocellular carcinoma or cholangiocarcinoma will require further characterisation with additional contrast enhanced cross-sectional imaging.

12.6 Portal Vein Gas

Gas within the portal vein is a rare finding on ultrasound and is associated with a number of conditions (Table 12.4), including bowel ischaemia, gastrointestinal sepsis and obstruction. Initially viewed as an imaging sign of mortal disease, there are increasing reports of reversible or more benign disease processes that can temporarily cause this phenomenon to be observed sonographically [14]. At

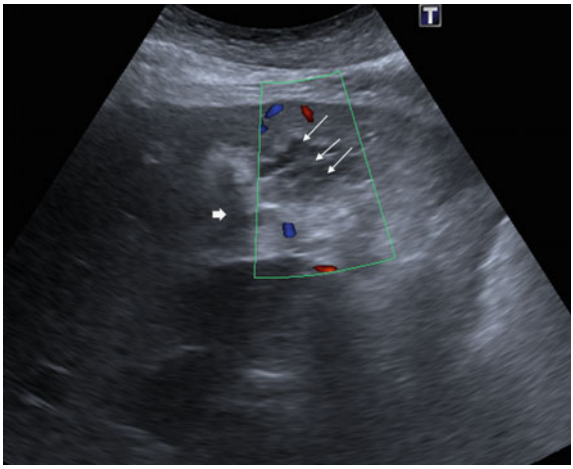

Fig. 12.24 Transverse view of the left liver, showing crowding of dilated ducts and port vein branches (arrows), due to atrophy of the left lobe. No flow is seen with any of these on Colour Doppler and the left portal vein (thick arrow), was also occluded. A central infiltrating mass was subsequently demonstrated on contrast ultrasound

Table 12.4 Conditions associated with portal vein gas [14]

Condition
Necrotising enterocoltis
Mesenteric artery occlusion
Hypertrophic pyloric stenosis
Ventral hernia Diverticulitis
COPD
Blunt abdominal trauma
Appendicitis
Crohn's disease Enterovascular fistula Perforated gastric ulcer Liver abscess

ultrasound tiny echogenic foci are seen to stream through the portal vein in the direction of portal vein flow, fanning out into periphery of the liver, causing multiple pinpoint echoes, which are more marked in the subscapular parenchyma. Spectral Doppler interrogation of the portal vein, will demonstrate thin spikes of high signal imposed on the normal portal vein trace and a distinctive cracking sound described as "the bubbling cauldron" (Fig. 12.25). This appearance can be distinguished from pneumobilia, which tends to be more central in its location in the liver and only moves with changes in patient position.

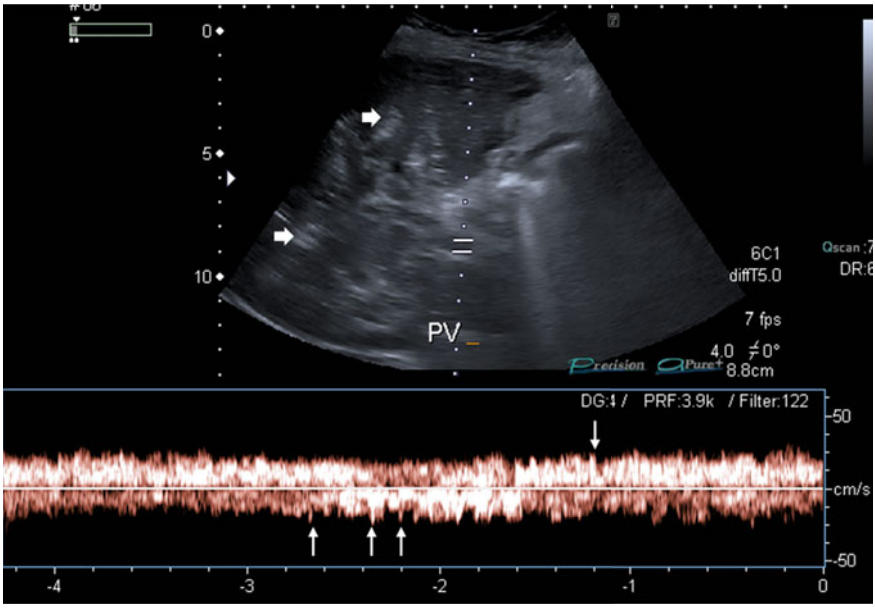

Fig. 12.25 Spectral Doppler trace of portal vein, showing multiple sharp spikes in the trace (arrows), due to portal vein gas. Branching echogenic regions are seen in the liver parenchyma (thick arrows) due to multiple gas interfaces

12.7 Portal Vein Occlusion

The two main causes for portal vein occlusion are thrombosis and tumour invasion, with the most common underlying pathology being portal hypertension secondary to cirrhosis. The more advanced the stage of cirrhosis the higher the risk for this complication to occur. In an acute thrombosis the portal vein may still appear anechoic and Doppler parameters will need to be optimised to ensure that there is not still very slow flow present: by reducing the Doppler scale, increasing the colour or spectral gain and if possible altering the Doppler frequency. If there is still uncertainty, then the use of an ultrasound contrast agent or contrast enhanced CT/MRI should be considered. In more chronic thrombosis the clot is more echogenic and may retract, with partial recanalization of the portal vein. A network of collaterals can develop around a chronically thrombosed main portal vein within a few weeks, seen on colour Doppler as a cluster of tortuous vessels, with continuous low flow entering the liver (Fig. 12.26).

Tumour thrombus tends to cause significant expansion of the involved portal vein and can be confirmed by the detection of arterial Doppler traces within the thrombus.

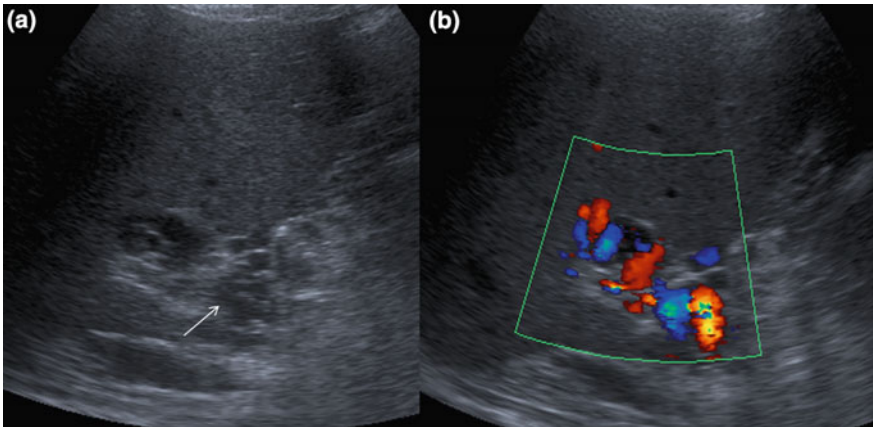

Fig. 12.26 **a** Longitudinal oblique view of the porta, showing a cluster of tortuous vessels at the hepatic porta indicated by serpiginous anechoic structures (arrow). **b** Colour Doppler confirms flow within these structures and absence of flow in the main portal vein, consistent with cavernous transformation

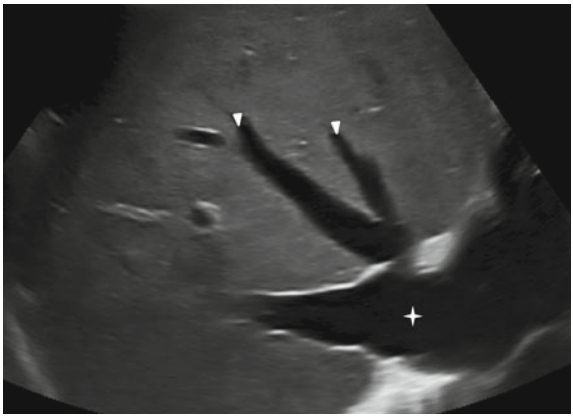

Fig. 12.27 Transverse view of liver showing dilated hepatic veins (arrowheads) at their confluence with the dilated IVC (star)

12.8 Hepatic Venous Congestion

Abnormal liver function tests are often found in patients with congestive cardiac failure due to passive hepatic venous congestion. Ultrasound of the liver will demonstrate dilatation of the hepatic veins, with no tapering of the veins at their confluence with the IVC (Fig. 12.27); this is best appreciated on a transverse view

through the liver at the hepatic vein confluence and has been referred to as "the playboy bunny sign" [15]. The retrohepatic IVC is also distended—adopting a rounded as opposed to oval contour on transverse scanning. The liver may be mildly enlarged and demonstrate increased periportal reflectivity.

12.9 Hepatic Venus Outflow Obstruction

In addition to hepatic venous congestion, veno-occlusive disease and Budd Chiari syndrome can also cause venous outflow obstruction and result in hepatomegaly. The former involves the venules at sinusoidal level, while in Budd Chiari the occlusion occurs at the level of the hepatic veins and/or the IVC between the liver and the right atrium, which can be acute or chronic. The findings at ultrasound therefore differ between these conditions. In veno-occlusive disease normal flow is seen on colour Doppler in the hepatic veins, but there may be reduced flow in the portal vein, with intermittent flow reversal, which may be confined to a single branch of the portal vein [16]. In acute Budd Chiari syndrome the liver may be enlarged, with enlarged proximal hepatic veins, or visible narrowing. Altered flow is demonstrated in the veins on spectral Doppler, with either a flat trace or reversal (i.e. towards the liver). With chronic disease, collateral veins may be seen between the main hepatic veins, either intrahepatic or subcapsular in location. The caudate lobe will frequently enlarge and can compress the IVC [17].

12.10 Spleen

12.10.1 Anatomy

The spleen lies in the left upper quadrant of the abdomen, with its long axis orientated along the line of the 10th rib. It has a smooth curved wedge shape, with the upper lateral convex wall in contact with the left hemidiaphragm. The concave side of the spleen has potential contact with the stomach, left kidney and flexure (splenic) of the colon. Within its concave face the splenic hilum is the vascular pedicle of the spleen, containing the artery, veins, lymphatics and nerves, with the tail of the pancreas lying along the line of the main splenic vein.

At ultrasound the convex surface of the spleen is smooth, while the concave surface may be more lobular, with the splenic hilum clearly appreciated by the entry and exit of relatively anechoic vascular structures, which can be confirmed using colour Doppler. The echotexture of the spleen is quite homogeneous, the reflectivity being slightly higher than the liver and visibly higher than the adjacent left kidney. The central artery of the spleen is seen to branch out forming the main segmental arteries; again this is better appreciated using colour or power Doppler (Fig. 12.28).

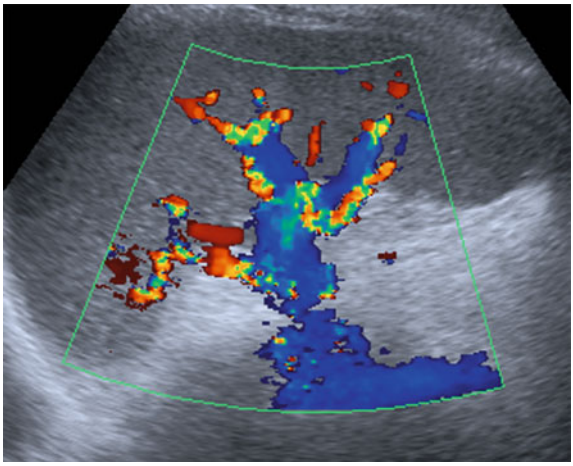

Fig. 12.28 Longitudinal view of the spleen showing normal arterial branching at the splenic hilum on colour Doppler (coded red)

10–30% of patients will have an accessory spleen (splenunculi), which failed to fuse with the main body of the spleen during its embryogenesis. At ultrasound these are seen as small (usually <2 cm) rounded or ovoid soft tissue masses, of similar echotexture to the main spleen. Most commonly these are closely related to the spleen or tail of the pancreas, but can lie elsewhere within the abdomen [18].

Rarely the spleen may lie in an unexpected location, including the pelvis. This wandering spleen is due to under development or elongation of its supporting ligaments and can result in misinterpretation of the spleen for an abdominal mass.

Another pitfall to be wary of is the adjacent stomach. In the presence of a gastric ileus or NG feed within the stomach, it can be misinterpreted at ultrasound for an air containing collection deep to or beyond the spleen (Fig. 12.29). Confirmation that

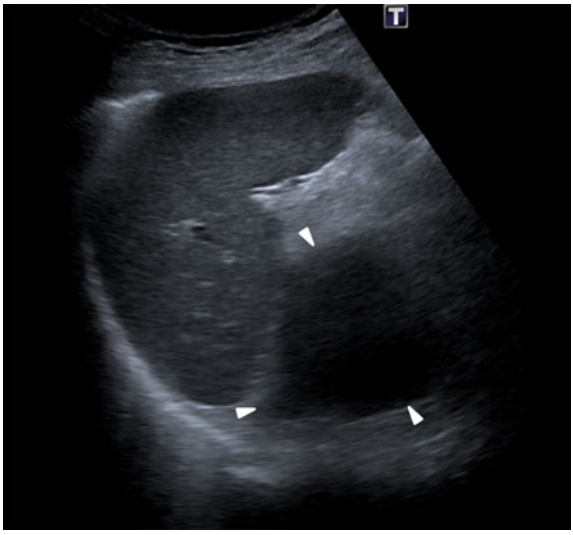

Fig. 12.29 Longitudinal oblique view through the spleen, with the stomach containing fluid and feed distal to this (arrowheads). This can be misinterpreted as a collection in the left upper quadrant

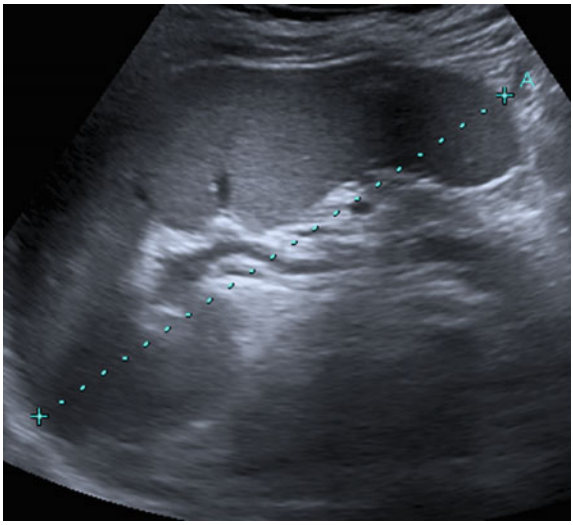

Fig. 12.30 Longitudinal view for measuring splenic length. The width can be measured by rotating the probe 90° clockwise for an anteroposterior measurement at the hilum

this is in fact the stomach can be made by scanning in the epigastric region, both in transverse and longitudinal plane.

12.10.2 Splenic Size

By placing the ultrasound probe within the 10th -11th intercostal space it should be possible to obtain a reasonable longitudinal image of the spleen, from which a splenic length and width measurement can be obtained (Fig. 12.30): sometimes this will require altering patient position as described above. Normal splenic length does vary according to patient age, sex, and body habitus, but a general rule of 12 cm as the upper limit of normal is usually accepted, with 12–13 cm seen as indeterminate and more than 13 cm (>5 cm antero-posterior width) enlarged. There are numerous causes of splenomegaly (Table 12.5) and it is usually not possible to identify the cause with ultrasound alone.

Splenic length <7 cm and width <3 cm is viewed as small, and may indicate functional hyposplenia [19].

12.10.3 Infarcts

Infarction of the spleen, may be either arterial or venous in origin, with haematological disorders a common cause in the younger patient and embolic events seen more in the older patient. Venous infarction may occur with portal or splenic vein

Table 12.5 Causes of splenomegaly

Pathological Process	Type	Example
Infection	***Viral***	Infectious mononucleosis, AIDS, CMV
	Bacterial	Tuberculosis, brucellosis, typhoid, Abscess
	Fungal	Histoplasmosis, candidiasis
	Protozoal	Malaria, Schistosomiasis, Leishmaniasis
Haemodynamic		Cirrhosis, Portal/Splenic vein obstruction, Budd Chiari, Right heart failure
Lymphohaematological	***Anaemias***	Sickle Cell, Thalassaemia, Spherocytosis, Pyruvate Kinase Deficiency,
	Myeloproliferative Lymphoma Leukaemia	Myelofibrosis, Polycythaemia Vera Hodgkin's Disease, Non-Hodgkins lyphoma Chronic Myeloid leukaemia, Chronic Lymphocytic leukaemia
Storage Diseases		Gaucher's disease, Niemann-Pick disease, Mucopolysaccharidoses
Connective Tissue		Rheumatoid arthritis, Systemic lupus Erythematosus
Neoplastic		Haemangioma, Lymphangioma, Angiosarcoma, Metastases
Trauma		Haematoma, Pseudocyst
Miscellaneous		Amyloid, sarcoid

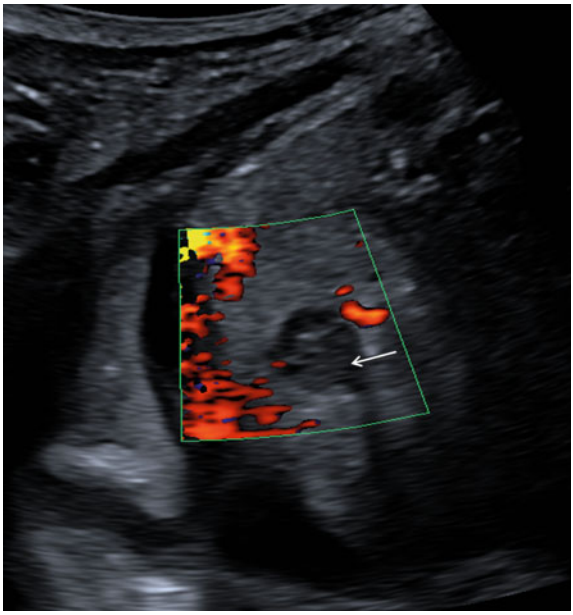

Fig. 12.31 Splenic infarct: Well circumscribed area of reduced reflectivity (arrow) in the spleen, with relatively straight margins and no associated power Doppler signal

thrombosis. It can be asymptomatic, present with left upper quadrant pain and sometimes fever, or other constitutional symptoms. Sonographically changes may not be apparent in the first 24 h. When visualised they are typically a peripherally based, wedge shaped region of reduced reflectivity, with the apex orientated towards the hilum of the spleen (Fig. 12.31). Colour Doppler can be helpful by confirming a segmental absence of blood flow in this region: although this is not always seen. Not all infarcts are wedge shaped however, with some taking on a rounded or oval contour, making it difficult to distinguish from other hypovascular splenic mass lesions. In these situations, the recognition of thin linear echogenic interfaces within the affected splenic tissue can increase operator confidence in diagnosing a focal infarct, rather than an alternative pathology [20]. As infarcts mature they tend to reduce in size, and become relatively echogenic with respect to the background spleen.

12.10.4 Abscess

Splenic abscesses are relatively rare and may be due to either bacterial, protozoal, or fungal agents. Bacterial infections are usually through haematogenous spread, but can also arise through direct spread of infection from adjacent organs (e.g. pancreas) or penetrating injury. The typical clinical presentation is with fever, left upper quadrant pain and a leucocytosis, but it can also be relatively asymptomatic, particularly in the immunocompromised patient. Sonographically abscesses can be single or multiple, with a variable appearance depending upon their aetiology. The typical appearance is of a rounded, but irregular thick-walled, low reflective, partially cystic lesion with some through transmission of sound seen in the splenic tissue beyond this. Rarely gas may be present within the abscess in which case there will be "dirty" acoustic shadowing beyond the strongly echogenic gas interface. Colour Doppler interrogation will typically show absence of any flow within the central component of the abscess.

In the immune compromised patient, involvement of the spleen by Mycobacterium tuberculosis or fungal infections such as Candida albicans can appear as multiple hypoechoic nodules [21, 22], which needs to be distinguished from lymphoma. Ultrasound findings in the rest of the abdomen can be helpful here, with the associated findings of ascites, intestinal wall thickening and lymphadenopathy suggestive of tuberculosis. Whereas Candida has a number of patterns in the spleen, most typically a 'wheel within a wheel' or 'bulls-eye' pattern, both of which demonstrate an echogenic centre to the hypoechoic nodule, the former with a further hypoechoic central nidus.

For both patterns of splenic abscess, diagnosis can be confirmed through ultrasound guided fine needle aspiration. For the larger focal abscess, percutaneous catheter drainage under ultrasound guidance is now the standard management approach rather than surgical intervention [23].

12.10.5 Cysts

Unlike the liver and kidneys splenic cysts are relatively uncommon and can be divided up into primary cysts, which include congenital cysts, parasitic cysts, cystic tumours, and secondary cysts or pseudocysts. True congenital cysts, also known as epidermoid cysts, are characterised by an inner endothelial lining and unless very large are usually an incidental finding. Typically, they are purely anechoic with a well-defined thin echogenic interface, best seen where the cyst wall is perpendicular to the ultrasound beam, and demonstrate posterior acoustic enhancement (Fig. 12.32). They can sometimes contain fine internal echoes from cholesterol crystals and thin echogenic septations have also been reported [24].

Parasitic cysts are usually due to hydatid disease, the majority due to infection by Echinococcus granulosusa which has a variety of appearances at ultrasound depending upon the stage of infection. The presence of multiple daughter cysts within the main cyst or a collection of central curvilinear echoes representing detached floating membranes are reported as pathognomonic for this condition [25].

Pseudocysts lack an epithelial lining and are either post-traumatic in aetiology, or are the sequela of previous infection or infarction. Usually they are sonographically indistinguishable from congenital cysts. The presence of wall calcification seen as echogenic foci, casting acoustic shadows, favours the diagnosis of a pseudocyst.

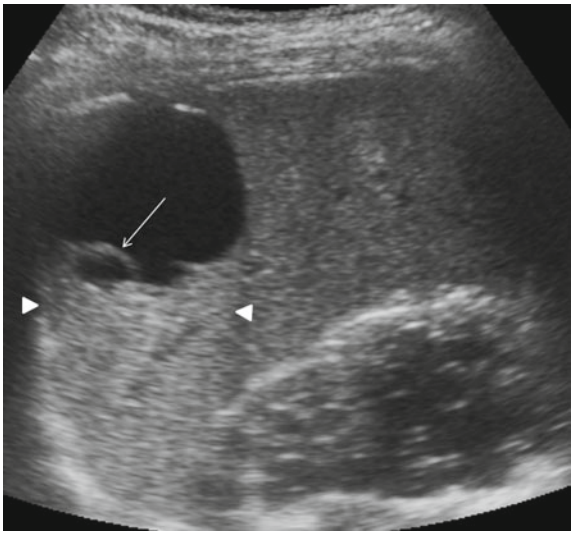

Fig. 12.32 Longitudinal view of the spleen, containing an anechoic, thin walled cyst, with a single echogenic septation (arrow). There is associated posterior acoustic enhancement (arrowheads), indicating likely fluid content

12.10.6 Focal Masses

Solid tumours of the spleen are rare, with benign lesions slightly more common. Uniformly echogenic solitary mass lesions <2 cm in size with mild posterior acoustic enhancement, can be assumed benign and are most likely cavernous or capillary haemangiomas [26, 27]. Atypical haemangiomas may be hypoechoic, partially cystic or contain shadowing echoes of calcification. These may require further characterisation with either contrast ultrasound [28] or MRI.

Lymphoma is the most common malignant tumour in the spleen and if detectable at ultrasound has a number of appearances including: multiple small or large hypoechoic nodules; infiltrating low reflective masses, or a more subtle diffuse alteration in splenic echotexture [29]. Multiple small echogenic nodules have also been rarely reported.

Metastases to the spleen are uncommon and primary non-lymphomatous malignancies of the spleen are exceptionally rare, both having variable appearances at ultrasound making accurate characterisation virtually impossible.

12.10.7 Rupture

Splenic rupture usually results from blunt abdominal trauma, but can occur through infection or haematological malignancy. In acute rupture of the spleen ultrasound can demonstrate fissures within the spleen as echogenic or low reflective clefts

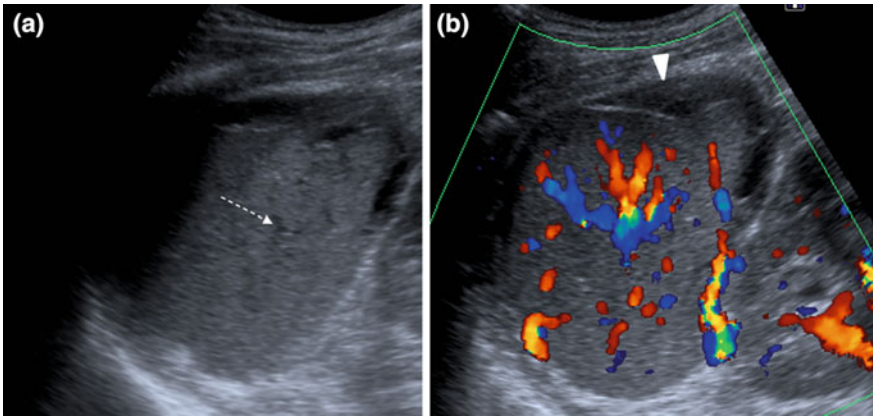

Fig. 12.33 Splenic trauma: **a** Longitudinal oblique view through traumatised spleen, with an irregular contour and low reflective lines within the parenchyma representing lacerations (dashed arrow). **b** Colour Doppler can help highlight perisplenic haematoma (arrowhead), through its lack of vascularity, as this can sometimes be isoechoic to the adjacent spleen

(Fig. 12.33) [30]. With increasing severity subcapsular haematomas of varying reflectivity are seen, which can be highlighted through colour Doppler, demonstrating the avascular rim of haematoma. Free fluid in the peritoneum is a non-specific finding indicating haemoperitoneum. Active haemorrhage is extremely difficult to demonstrate, even with colour Doppler, but post traumatic pseudoaneurysms can be seen as a rapidly alternating colour flow pattern, inside a cystic like space. The primary assessment of splenic trauma however remains contrast enhanced CT.

12.11 Gallbladder and Bile Ducts

Ultrasound is the first line imaging investigation for patients on ICU with jaundice, right upper quadrant pain or suspected sepsis/inflammation of the biliary tree. Careful systematic examination of the gallbladder, common bile duct and intrahepatic bile ducts may reveal gallbladder wall thickening, gallstones or sludge within the lumen, a peri-cholecystic collection suggesting perforation, or dilation of the common and or intra-hepatic ducts due to an intraluminal obstruction or from extrinsic compression.

12.11.1 Anatomy

The intrahepatic bile ducts run in the portal tracts of the liver, parallel to the portal vein radicals, and at the porta hepatis the right and left hepatic ducts join to form the common hepatic duct. This lies anterior to the main portal vein and continues inferiorly for about 3 cm before the cystic duct, from the gallbladder, joins it to form the common bile duct. The common bile duct then continues caudally, positioned anterior to the lateral margin of the portal vein, with the hepatic artery medial to it. It enters the head of the pancreas, where it turns laterally to drain into the second part of the duodenum, accompanied by the pancreatic duct.

The gallbladder is a pear-shaped reservoir, measuring 8–12 cm in length, with a thin wall (2 mm) made up of a mucosal lining, fibromuscular layer and serosal surface. It lies in a fossa on the under surface of the right lobe of the liver, with the distal fundus often projecting below the inferior margin of the liver. The proximal neck of the gallbladder curves back round on itself, heading caudally to become the cystic duct. This latter structure contains a number of mucosal folds—spiral valves—which can cast acoustic shadows at ultrasound, potentially mimicking calculi.

On ultrasound, the normal right and left hepatic ducts are visible as anechoic tubular structures, lying anterior to the right and left portal veins and measuring up to 2 mm in diameter. The more peripheral intrahepatic ducts are often too small to resolve. The common hepatic duct is usually seen on a right longitudinal oblique

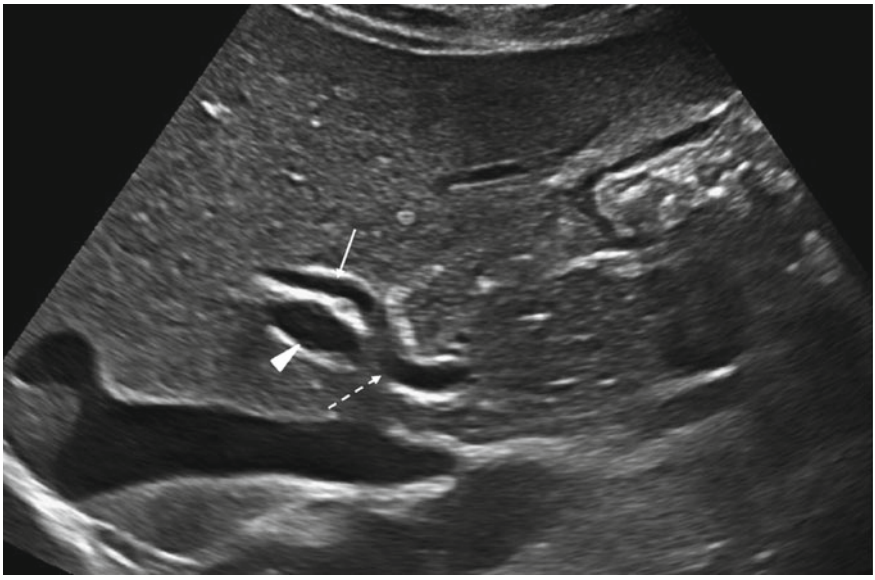

Fig. 12.34 Longitudinal oblique view of the porta, with the common hepatic duct (arrow) seen adjacent to the portal vein (arrowhead). Beyond the porta, where the duct tends to bend (dashed arrow), it is usually referred to as the common bile duct

view of the porta, measuring up to 5 mm (inner wall to inner wall) (Fig. 12.34). It is often difficult on ultrasound to determine the junction with the cystic duct, but beyond the porta the duct is generally assumed to represent the common bile duct; here it is allowed to measure up to 6 mm. In the elderly patient small increases in common duct diameter may be seen, although it should still remain below 6–7 mm

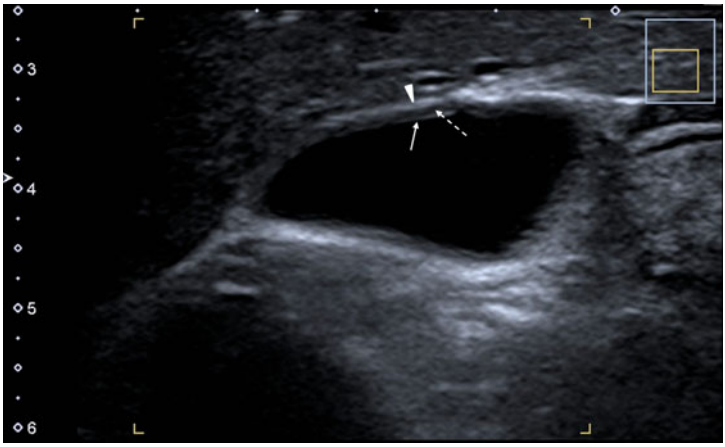

Fig. 12.35 Zoomed image of partially contracted gallbladder, with the mucosal interface (arrow), muscle wall (dashed arrow) and serosal interface (arrowhead) seen as three distinct layers

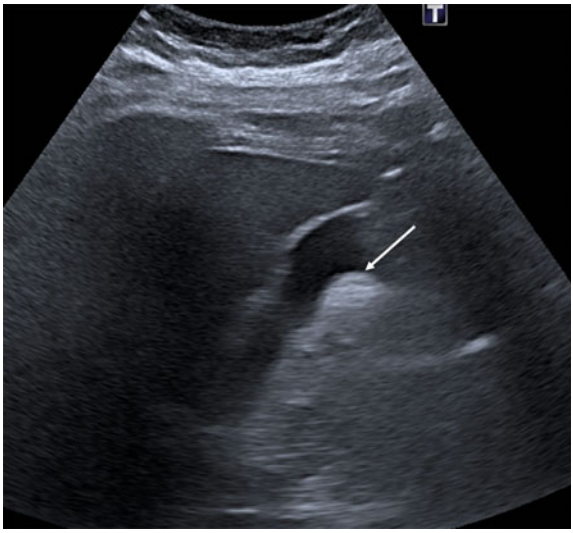

Fig. 12.36 Oblique longitudinal view through the gallbladder. In this rather limited view, gas within the duodenum (arrow) is seen as a rounded echogenic area that appears to lie within the gallbladder lumen and could be mistaken for a gallstone

[31]. Post cholecystectomy the common bile duct may increase in calibre, with acceptable limits up to 1 cm.

In the fasting state, the gallbladder lumen is anechoic and the wall is seen as a single echogenic interface, measuring <3 mm. This is best measured on a true longitudinal image of the gallbladder, from the anterior wall. Care should be taken to ensure the wall is truly perpendicular to the ultrasound beam to avoid artefactual thickening. There maybe be infolding of the wall of the gallbladder (mucosal folds), usually seen at the neck of the gallbladder or fundus, which can lead to interpretation errors. When contracted, the gallbladder wall has three visible layers, an outer and inner echogenic interface and a low reflective layer in between (Fig. 12.35).

In some patients the closely related duodenum can indent the posterior wall of the gallbladder, with echogenic gas in the duodenum giving the impression of gallbladder pathology (Fig. 12.36). Repositioning the patient, changing scanning approach or introducing some fluid into the duodenum can help clarify this, where there is uncertainty.

12.11.2 Gallbladder Thickening

A gallbladder wall thickness of >3 mm is considered abnormal in the normal fasting gallbladder: although measurements between 3 and 4 mm are viewed as indeterminate in their significance. Measuring the wall thickness in the transverse plane is not recommended, to avoid artefactual thickening of the anterior wall through scanning obliquely (Fig. 12.37). At the same time as measuring the wall thickness, assessment can be made for any evidence of gallbladder wall tenderness by gentle probe compression.

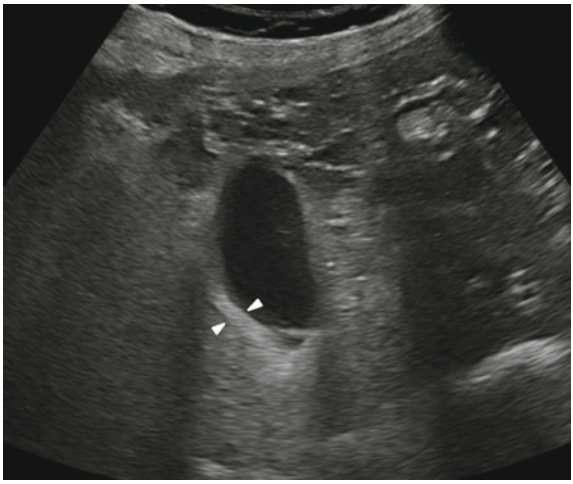

Fig. 12.37 An oblique transverse view through the gallbladder, demonstrating how the gallbladder wall can appear thickened (arrowheads). Subsequent longitudinal views confirmed normal wall thickness

Table 12.6 Causes of diffuse and focal gallbladder wall thickening

Diffuse	Focal
Physiological: Post Prandial **Cholecystitis**: Acute Chronic Gallbladder empyema Xanthogranulomatous Acalculous	**Polyps**: Cholesterol Adenomatous **Malignancy**: Gallbladder Carcinoma Metastases (rare) Focal Adenomyomatosis Focal Xanthogranulomatosis Adherent Gallbladder Sludge (pseudo-focal thickening)
Adjacent Inflammation: Hepatitis Pancreatitis Severe Pyelonephritis Colitis **Systemic**: Cardiac failure Renal failure Hypoalbuminaemia Sepsis **Hypertrophic:** Adenomyomatopsis **Malignancy**: Gallbladder Carcinoma Lymphoma	

The thickened gallbladder usually demonstrates a 3-stripe layer, with a central low reflective echo. Depending upon the underlying pathology, there may also be pericholecystic fluid or ascites present. In addition to acute or chronic inflammation, gallbladder wall thickening can be a result of non-biliary disease processes

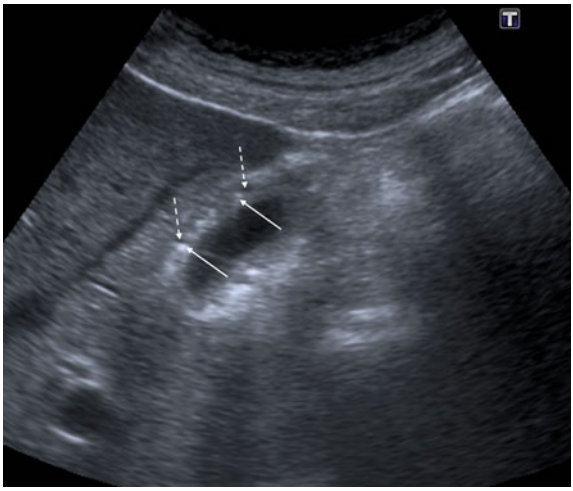

Fig. 12.38 Oblique longitudinal view of a partially contracted gallbladder, showing multiple echogenic foci in the anterior wall (arrows), some demonstrating comet tail artefact and associated cystic spaces (dashed arrows), typical for adenomyomatosis

including renal failure and AIDS [32]. There are a number of causes for gallbladder wall thickening which are listed in Table 12.6.

Focal thickening of the gallbladder wall can be seen in adenomyomatosis, where regional mucosal hyperplasia results in the development of intramural diverticular lined by mucosa: the Rokitansky-Aschoff sinus. Usually affecting the fundus of the gallbladder, these are seen on ultrasound as either tiny cystic spaces in the thickened wall, or if they contain cholesterol crystals/bile salts, tiny echogenic foci, with associated comet tail artefact (Fig. 12.38) [33].

12.11.3 Stones, Polyps and Sludge

At ultrasound the gallbladder lumen may contain: anechoic bile; echogenic bile salts; focal echogenic structures representing stones or polyps; or fine echoes from haemorrhage or biliary sludge.

Ultrasound is considered the gold standard test for gallstones, with sensitivity for their detection around 96%. Gallstones are typically seen as strongly echogenic, intra-luminal mobile structures that cast acoustic shadows (Fig. 12.39). The acoustic shadow seen with gallstones differs to that produced by bowel gas in the adjacent duodenum, having a much more defined edge and lacking internal echoes from reverberation. This is because the incident ultrasound beam is mainly absorbed by the stone rather than reflected, as it is at an air interface [34]. The acoustic shadowing artefact from gallstones can be enhanced by adjusting the focal zone to lie at the level of the stones, scanning using the highest frequency possible and altering the angle of insonation to a more perpendicular approach. Some small cholesterol stones (<3 mm) however may not cast acoustic shadows and in this situation, demonstrating their mobility is important to make the distinction between

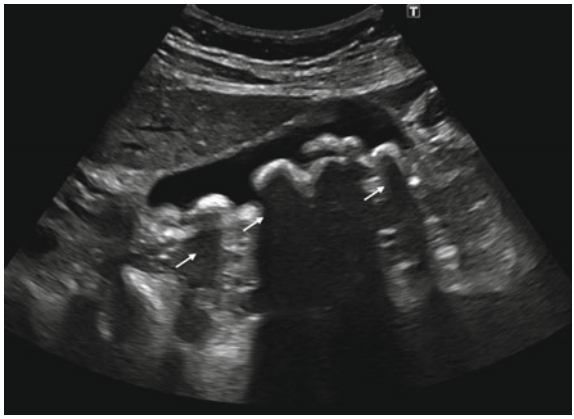

Fig. 12.39 Longitudinal oblique view through gallbladder, with normal wall thickness. Multiple gallstones are present casting several acoustic shadows (arrows)

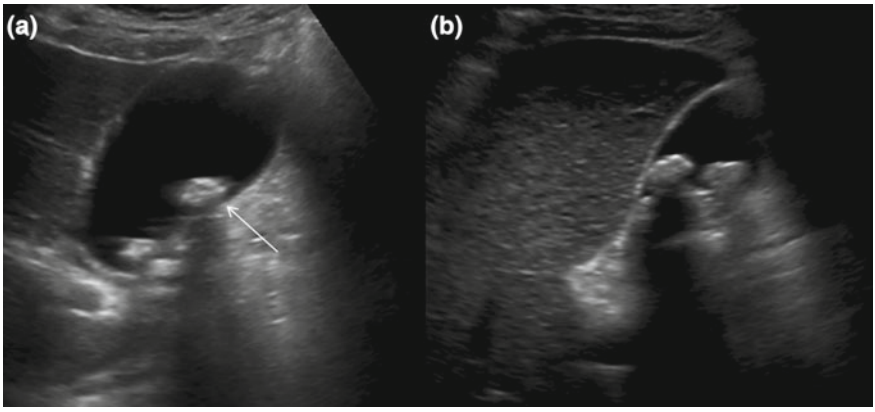

Fig. 12.40 **a** Supine position, dependent gallstones (arrow) along posterior GB body. **b** Left lateral decubitus position, gallstones have moved position, bunched up at GB neck

a stone and a gallbladder polyp. This often requires moving the patient, either onto their left side or even semi-prone and then repeating the scan to demonstrate a change in position of the stone (Fig. 12.40). Sometimes the gallbladder will be packed with stones and contracted, so that all that is appreciated at ultrasound within the gallbladder fossa is a double echogenic arc, representing the gallbladder wall and layer of stones, with an associated strong acoustic shadow. In this situation careful scanning of the gallbladder fossa from different planes is required to distinguish this from adjacent bowel (Fig. 12.41).

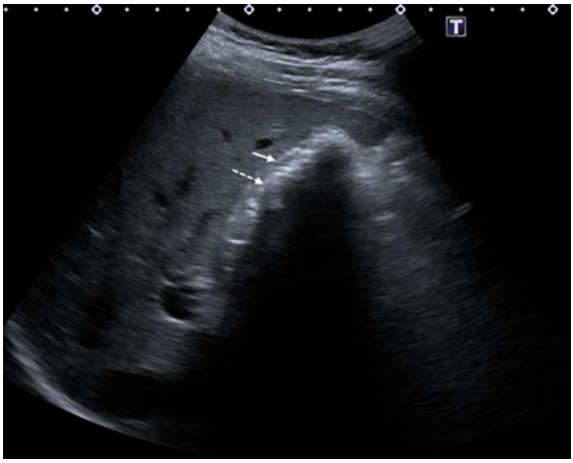

Fig. 12.41 Oblique longitudinal view of the gallbladder, which is packed with stones, giving a "double arc" echogenic interface. The outer arc (arrow) represents the gallbladder wall and the inner (dashed arrow) the gallstones. This is also known as the "wall-echo-shadow" sign, with the "shadow" referring to the acoustic shadow from the gallstones

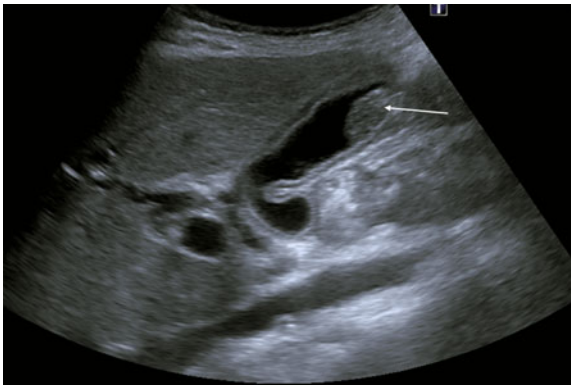

Fig. 12.42 Oblique longitudinal view of the gallbladder, with an apparent echogenic mass in the fundus (arrow), which was confirmed as sludge on MRI

Gallbladder polyps are the main differential at ultrasound for gallbladder stones and are relatively common, with a reported incidence of up to 6.9% [35]. These are mainly cholesterol polyps, which are typically multiple, <10 mm in size and can cast a faint acoustic shadow at ultrasound. Their lack of mobility or attachment to the anterior wall of the gallbladder is often their only distinguishing feature from a stone at ultrasound. True adenomatous polyps are much less common, are usually solitary and are either sessile or pedunculated in shape. While cholesterol polyps are truly benign, adenomatous polyps are viewed as having malignant potential and ultrasound follow-up of these may be required, depending upon polyp size, its contour and the patient's age.

Biliary sludge or echogenic bile is a common finding in the ICU patient, due to biliary stasis. This represents precipitates of calcium salts and cholesterol crystals, which usually form a dependent layer in the gallbladder lumen, but can on occasion

aggregate to form a sludge ball that can mimic a gallbladder wall mass (Fig. 12.42). Demonstrating flow or movement of the sludge to separate these possibilities is not always clear, as it can be extremely viscid: in which case repeating the ultrasound after the patient has left ITU should confirm resolution of this finding.

Echogenic bile may also be seen when there is blood or pus in the gallbladder lumen and the clinical presentation, history (any recent intervention or trauma), is key to making this distinction.

12.11.4 Acute Cholecystitis

Usually as a result of gallbladder obstruction from a gallstone, the sonographic findings in acute cholecystitis can be variable. The described "major" diagnostic findings are: the presence of gallstones in the gallbladder (a stone may be seen in the cystic duct), gallbladder wall oedema, gas in the gallbladder wall and visible patient discomfort, when the ultrasound probe directly overlies the gallbladder (sonographic Murphey's sign) [36]. Less specific—"minor"- findings include: pericholycystic fluid, wall thickening, increased distention and luminal changes (i.e. sludge, stranding across lumen). A combination of major and minor findings at ultrasound, can give a diagnostic sensitivity for cholecystitis of up to 90–98% and a specificity of 94–98% [37].

Gallbladder wall oedema is seen on ultrasound as a thickening of the low reflective central zone of the wall, which if marked can take on a stratified appearance (Fig. 12.43), or as an echo- poor halo around the gallbladder. Increased mural blood flow along the anterior wall may be seen on colour Doppler, although as a diagnostic finding for cholecystitis this is relatively non-specific: particularly with modern ultrasound systems which can demonstrate the cystic artery in normal gallbladders [38].

As well as confirming a suspected diagnosis of cholecystitis, ultrasound can detect the possible complications that can occur, including empyema, gangrenous cholecystitis, perforation, pericholecystic collections and emphysematous cholecystitis. Gallbladder empyema has a non-specific finding of echogenic "sludge like"

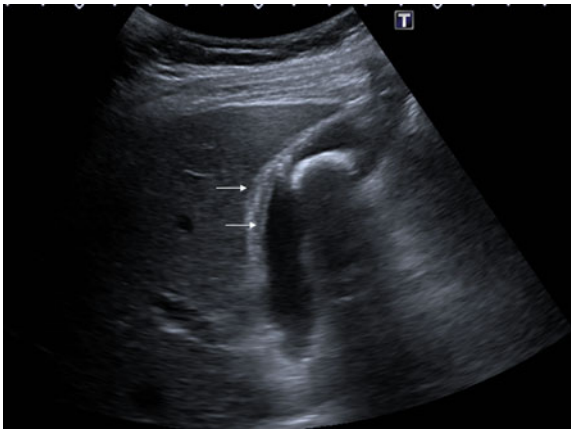

Fig. 12.43 Longitudinal oblique view of an inflamed gallbladder containing a gallstone. There is thickening and stratification of the gallbladder wall, with alternating hypoechoic (arrows) and echogenic lines, consistent with gallbladder wall oedema

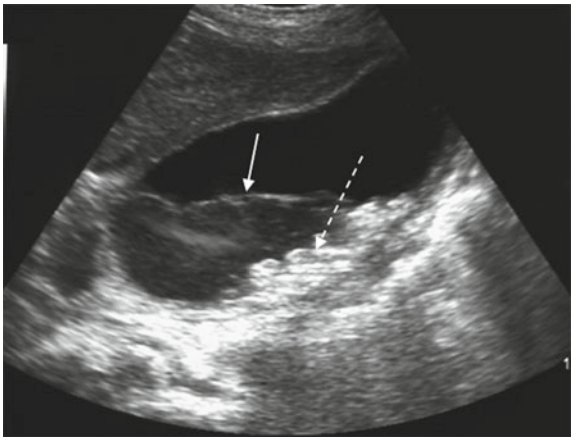

Fig. 12.44 Longitudinal oblique view of a thick-walled gallbladder with stones (dashed arrow) and layered material (arrow), which is suggestive of pus in keeping with empyema

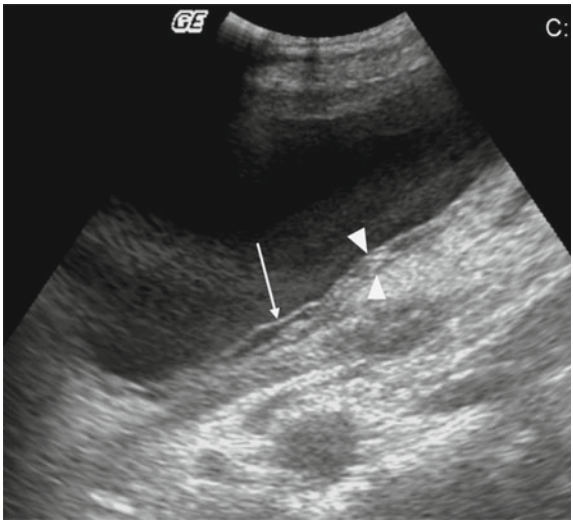

Fig. 12.45 Longitudinal view of an irregularly thickened (arrowheads) gallbladder wall, with a separated linear interface (arrow), very suggestive for mucosal separation, due to developing gangrenous cholecystitis

material, which is typically dependent in location (Fig. 12.44). With the onset of gangrenous change, irregular thickening of the gallbladder wall at ultrasound reflects the intramural haemorrhage, abscess formation and necrosis occurring. Intraluminal echogenic strands may be seen, representing fibrinous debris and mucosal sloughing (Fig. 12.45). With the onset of gangrene, the sonographic Murphy's sign will usually be negative, due to denervation of the gallbladder. Gallbladder perforation occurs in 5–10% of cases of cholecystitis and is a significant risk in gangrenous cholecystitis. It can be acute, sub-acute or chronic, with differing findings at ultrasound. Sub-acute perforation results in either pericholecystic fluid collections or frank abscess formation; which can be either predominantly echogenic, or a complex pattern of anechoic fluid with echogenic septations,

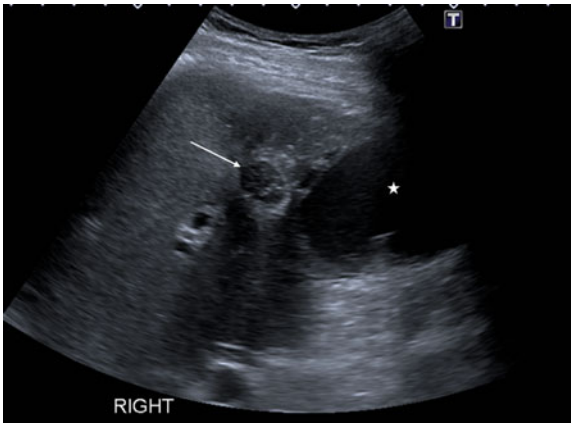

Fig. 12.46 Oblique view through the gallbladder fossa showing an inflamed gallbladder (star), with an adjacent oval shaped, intrahepatic collection/abscess (arrow)

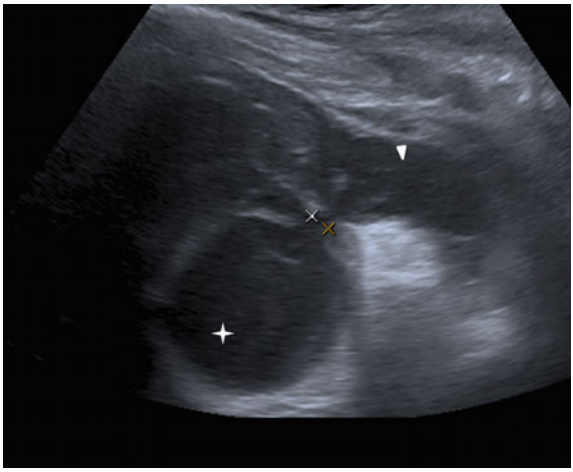

Fig. 12.47 Perforated gallbladder (star). Transverse view showing a focal defect of gallbladder wall (crosshairs) known as the "hole sign", with an adjacent collection (arrowhead)

although both will typically demonstrate through transmission of sound. Abscess formation may sometimes be seen within the adjacent liver (Fig. 12.46) rather than gallbladder fossa and pericholecystic fluid collections can also be seen secondary to pancreatitis, peritonitis or duodenal perforation. Careful interrogation of the gallbladder wall, in both transverse and longitudinal plane, may identify a perforation as a focal defect within the wall of the gallbladder: the hole sign (Fig. 12.47).

Gas in the gallbladder wall is the result of proliferating anaerobic infection (e.g. Clostridium) and is a potentially life threatening complication in cholecystitis, merited as a surgical emergency. More commonly seen in diabetic patients, approximately 30% of cases of emphysematous cholecystitis occur in the absence of gallstones. Mural gas formation is seen as focal, non-dependent echogenic areas in a thickened gallbladder wall, with comet-tail and ring down artefact within an acoustic shadow. If there is gas within the gallbladder lumen, it may be difficult to

discern the gallbladder as being separate to adjacent gas filled bowel, as it displays a diffuse linear echogenic interface and posterior acoustic shadowing containing internal reverberations. Changing patient position can help to confirm the gallbladder as separate from adjacent bowel and any gas within its wall may be seen to move with gravity [39]. If there is any doubt over the diagnosis, CT will confirm the presence of mural gas and distinguish this from calcification (i.e. porcelain gallbladder), which is the main differential for the appearances described.

Acalculous cholecystitis is gallbladder inflammation in the absence of gallstones, it accounts for about 10% of all cases of cholecystitis and typically occurs in hospitalised patients who are acutely ill or have undergone major surgery. Although the histological changes in the gallbladder are similar to gallstone cholecystitis, the pathogenesis is unclear, with a much higher incidence of gangrenous change and perforation. At ultrasound the lack of gallstones contributes to diagnostic difficulty, but gallbladder wall thickening, with hypoechoic regions and pericholecystic fluid are reported as the two most reliable findings [40]. The gallbladder may also contain echogenic sludge. In uncertain cases, a repeat ultrasound at 24 h may be helpful in demonstrating progression of changes. Ultrasound can also guide percutaneous aspiration of gallbladder contents for microbiology, although this has a recognised false negative rate [41].

12.12 Jaundice: Biliary Dilatation

In additional to the haematological and biochemical workup of the jaundiced patient, ultrasound has a key imaging role. It can sometimes detect a hepatocellular cause for the jaundice, such as underlying cirrhosis, malignant infiltration or an inflammatory process such as a liver abscess. However it is in the detection of biliary duct obstruction that ultrasound demonstrates a high level of accuracy; 80–85% in cases of proven obstruction, with a false positive rate of less than 5% [42–44].

Depending upon its aetiology, bile duct dilatation either affects the intrahepatic bile ducts, the extrahepatic ducts (common hepatic and common bile duct), or both. Levels of potential obstruction can be divided into hilar or porta hepatis, suprapancreatic and pancreatic; with ultrasound being able to correctly identify the level of obstruction in 92–95% of the time [45]. Obstruction at the hilar/porta hepatis is usually due to malignancy, most frequently cholangiocarcinoma and less commonly malignant lymphadenopathy.

Early or mild intrahepatic duct dilatation is best appreciated by scanning near the porta and assessing the diameter of the main right and left hepatic ducts. As already stated, these are normally <2 mm in diameter, while the more peripheral ducts should be <40% of the adjacent portal vein branch. With increasing duct dilatation the appearance in the liver has been described as the double channel or double-barrelled shot gun sign, depending upon the plane of scanning (when scanned along their length the dilated duct and adjacent portal vein appear as two

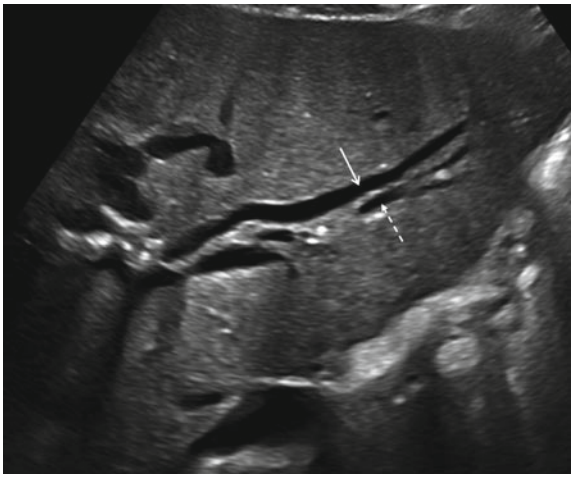

Fig. 12.48 Double barrelled shotgun sign: View through the left lobe of the liver, showing a portal vein branch (arrow) and adjacent dilated intrahepatic bile duct (dashed arrow)

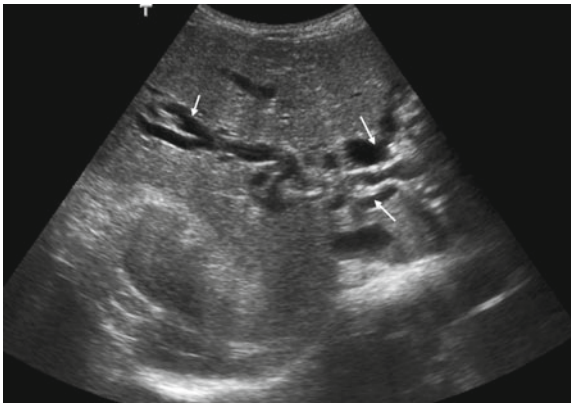

Fig. 12.49 Transverse view left lobe of liver with intrahepatic bile duct dilation (arrows), due to a cholangiocarcinoma of the common bile duct. Typical serpiginous branching pattern of tubular structures

channels, while in cross-section they are seen as if looking into a double-barrelled shot gun) (Fig. 12.48). At this degree of dilatation care must be taken not to mistake an enlarged segmental hepatic artery, associated with portal hypertension or portal vein occlusion, for bile duct dilatation and the use of colour Doppler to confirm absence of pulsatile flow can be useful. With established intrahepatic bile duct dilatation, the appearance seen at ultrasound is that of 'too many tubes' within the liver: the dilated ducts having an irregular/tortuous contour to them, and converge towards the porta to give a 'stellate pattern' (Fig. 12.49). As already stated, obstruction by an intrahepatic malignancy may appear as an abrupt cut-off of bile ducts, with the actual tumour difficult to discern on a non-contrast ultrasound. Obstruction at the porta due to periportal lymph nodes will usually show multiple oval or rounded hypoechoic masses in line with the portal vein.

Pitfalls can occur in early intrahepatic biliary obstruction, when they may have not been time for the ducts to dilate yet and in this situation repeat interval scanning is recommended, if there is strong clinical suspicion [46]. Segmental bile duct dilatation within the liver, due to a localised stricture or occluding mass, can be overlooked, without a careful segmental approach to assessing the liver parenchyma. Blood or debris within the bile ducts will make them relatively isoechoic to the liver parenchyma and may therefore mask dilatation. Non-obstructive bile duct dilatation can be seen in patients following biliary surgery, such as a biliary-enteric anastomosis.

Suprapancreatic obstruction is again most likely due to a primary neoplasm or metastatic disease, with gallstones or an inflammatory stricture much less likely. Rarely obstruction at this level can occur from a gallstone lodged in the cystic duct or neck of the gallbladder, leading to inflammatory swelling and extrinsic compression of the common bile duct or common hepatic duct, known as Mirizzi's syndrome. Ultrasound can confirm the presence of a stone within the cystic duct and demonstrate dilatation of the common hepatic duct proximal to this [47].

When bile duct dilatation is encountered on ultrasound, the gallbladder should be assessed for any degree of distention as this can sometimes aide in determining the level of obstruction. A distended gallbladder would suggest a low common duct obstruction, while a contracted gallbladder would tend to place the level of obstruction proximal to the cystic duct confluence within the common hepatic duct (Fig. 12.50). If the obstruction is due to gallstones however, this cannot be relied upon as previous episodes of gallstone cholecystits may have rendered the gallbladder fibrotic and unable to distend.

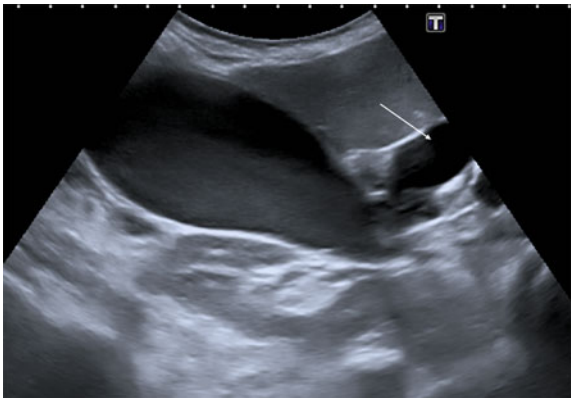

Fig. 12.50 Longitudinal view of a markedly distended gallbladder, in a patient presenting with jaundice. There is layering of echoes within the gallbladder lumen as a result of obstruction with a dilated common hepatic duct seen within the porta (arrow)

Obstruction at pancreatic level is the most common site of obstruction and can be due to gallstones, inflammatory strictures or masses and benign or malignant neoplasms. With careful technique and good equipment, the sensitivity of ultrasound for choledocholithiasis is between 75 and 82% [48]. This reduced sensitivity, compared to stones in the gallbladder, can be due to a number of factors: acoustic shadowing from gas in the adjacent duodenum can obscure the distal common duct; in early or intermittent obstruction the bile duct may not be significantly dilated, resulting in a lack of surrounding echo free bile, which normally helps highlight the relatively echogenic stone; around 10% of bile duct stones lack an acoustic shadow making these stones difficult to distinguish from other bile duct content such as sludge. Air within the common duct due previous sphincterotomy or gallstone complication (see below), may lead to a false positive diagnosis.

A tumour of the distal bile duct may be seen as a low reflective irregular mass, or as an abrupt, shouldered stricture of the distal duct, with a soft tissue tubular shaped structure distal to this. Malignant masses arising in the head of the pancreas will also lead to distal bile duct obstruction and are generally low reflective mass lesions with respect to the adjacent pancreatic tissue.

12.13 Pneumobilia

Gas/air in the bile ducts can be secondary to a surgical biliary—enteric anastomosis or fistula, biliary stent, incompetent sphincter of Oddi, erosion of a gallstone into the duodenum, or perforation of a duodenal ulcer into the common bile duct. At ultrasound, the intra hepatic or common bile duct lumen is obscured by either short echogenic segments, or longer branching linear echogenic foci, which may cast acoustic shadows, comet tail or ring down artefacts (Fig. 12.51). In the supine patient the air preferentially collects in the more anterior intrahepatic ducts within

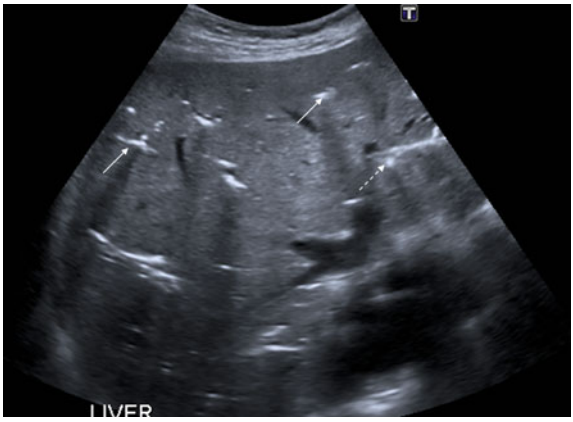

Fig. 12.51 Transverse scan through the right liver showing pneumobilia. There are numerous strongly reflective linear structures, representing bile ducts containing air/gas. Sone cast acoustic shadows (arrows), others generate comet tail or ring down artefact (dashed arrow)

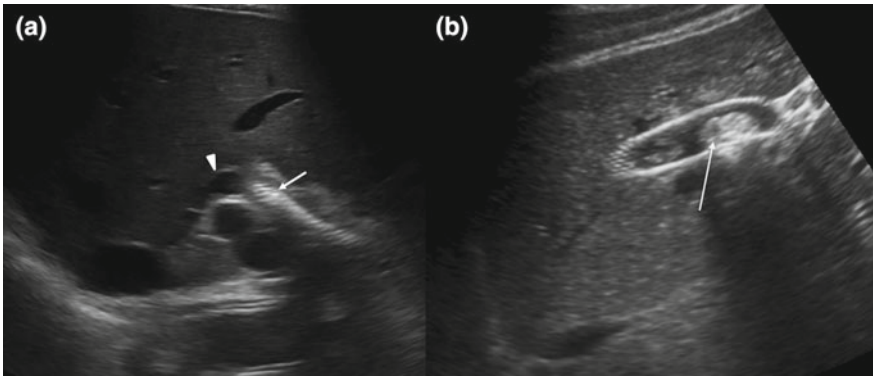

Fig. 12.52 Stent occlusion: **a** Hatched linear echogenicity at the porta hepatis indicates the position of a common bile duct stent (arrow). The common hepatic duct is dilated (arrowhead) and lacks pneumobilia indicating stent malfunction/occlusion. **b** Echogenic filling defects within the lumen of a malfunctioning intrahepatic stent (arrow) consistent with sludge. Again, the lack of pneumobilia indicates stent occlusion

the left lobe of the liver and in certain circumstances movement of the air can be appreciated as a flickering in the ring down/comet tail artefact. Small discrete foci of air can sometimes cast a 'clean' shadow mimicking a bile duct calculus.

In patients with a known biliary stents in situ, the absence or relative paucity of air with the intrahepatic bile ducts is strongly suggestive of stent malfunction (Fig. 12.52)

12.14 Cholangitis

Acute or ascending cholangitis has the reported triad of: fever, right upper quadrant pain and jaundice, although in reality this is seen in <40% of patients, with acute confusion and haemodynamic collapse another reported presentation. It is almost always associated with biliary obstruction, most commonly bile duct calculi, but also pre-existing bile duct strictures, malignant biliary obstruction or previous biliary surgery and interventional procedures. At ultrasound, biliary dilatation is a common finding and the level of obstruction can usually be determined with ultrasound. Purulent bile will produce echogenic debris within the bile ducts and there may be concordant intraductal calculi present. Thickening of the walls of the bile ducts tends to be seen with more chronic or recurrent episodes of cholangitis. Intrahepatic abscesses are not infrequently seen with acute cholangitis and ultrasound can be used to guide percutaneous aspiration of these and if there is obstruction percutaneous drainage of the biliary system.

References

1. Nicolaou S, Talsky A, Khashoggi K, Venu V. Ultrasound-guided interventional radiology in critical care. Crit Care Med. 2007;35(5 Suppl):S186–97.
2. Middleton WD, Melson GL. Diaphragmatic discontinuity associated with perihepatic ascites: a sonographic refractive artefact. Am J Roentgenol. 1988;151:709–11.
3. Le Couinaud C. foie: etudes anatomiques et chirurgicales. Paris: Masson; 1957.
4. Sidhu PS, Chong WK. Measurement in ultrasound: a practical handbook. London: Arnold; 2004.
5. Scatarige JC, Scott WW, Donovan PJ, Siegelman SS, Sanders RC. Fatty infiltration of the liver: ultrasonographic and computed tomographic correlation. J Ultrasound Med. 1984;3:9–14.
6. Jüttner HU, Ralls PW, Quinn MF, Jenney JM. Thickening of the gallbladder wall in acute hepatitis: ultrasound demonstration. Radiology. 1982;142:465–6.
7. Kuligowska E, Connors SK, Shapiro JH. Liver abscess: sonography in diagnosis and treatment. AJR Am J Roentgenol. 1982;138:253–7.
8. Hui JY, Yang MK, Cho DH, Li A, Loke TK, Chan JC, Woo PC. Pyogenic liver abscesses caused by Klebsiella pneumoniae: US appearance and aspiration findings. Radiology. 2007;242:769–76.
9. Vassiliades VG, Bree RL, Korobkin M. Focal and diffuse benign hepatic disease: correlative imaging. Semin Ultrasound CT MR. 1992;13:313–35.
10. Liu GJ, Lu MD, Xie XY, Xu HX, Xu ZF, Zheng YL, Liang JY, Wang W. Real-time contrast-enhanced ultrasound imaging of infected focal liver lesions. J Ultrasound Med. 2008;27:657–66.
11. Cai YL, Xiong XZ, Lu J, Cheng Y, Yang C, Lin YX, Zhang J, Cheng NS. Percutaneous needle aspiration versus catheter drainage in the management of liver abscess: a systematic review and meta-analysis. HPB (Oxford). 2015;17:195–201.
12. Gandolfi L, Leo P, Solmi L, Vitelli E, Verros G, Colecchia A. Natural history of hepatic haemangiomas: clinical and ultrasound study. Gut. 1991;32:677–80.
13. Ebara M, Ohto M, Shinagawa T, Sugiura N, Kimura K, Matsutani S, Morita M, Saisho H, Tsuchiya Y, Okuda K. Natural history of minute hepatocellular carcinoma smaller than three centimeters complicating cirrhosis. A study in 22 patients. Gastroenterology. 1986;90:289–98.
14. Huang C-Y, Sun J-T, Tsai K-C, Wang H-P, Lien W-C. Hepatic portal venous gas: review of the literature and sonographic implications. J Med Ultrasound. 2014;22:66–70.
15. Hokama A, Arakaki S, Shibata D, Maeshiro T, Kinjo F, Fujita J. "Playboy Bunny" sign of congestive heart failure. West J Emerg Med. 2011;12:433–4.
16. Yoshimoto K, Ono N, Okamura T, Sata M. Recent progress in the diagnosis and therapy for veno-occlusive disease of the liver. Leuk Lymphoma. 2003;44:229–34.
17. Ralls PW, Johnson MB, Radin DR, Boswell WD, Lee KP, Halls JM. Budd-Chiari syndrome: detection with color Doppler sonography. AJR Am J Roentgenol. 1992;159:113–6.
18. Mortelé KJ, Mortelé B, Silverman SG. CT features of the accessory spleen. AJR Am J Roentgenol. 2004;183:1653–7.
19. Görg C1, Eichkorn M, Zugmaier G. The small spleen: sonographic patterns of functional hyposplenia or asplenia. J Clin Ultrasound. 2003; 31(3):152–5.
20. Llewellyn ME, Brooke Jeffrey R, DiMaio MA, Olcott EW. The sonographic "Bright Band Sign" of splenic infarction. J Ultrasound Med. 2014;33:929–38.
21. Sharma SK, Smith-Rohrberg D, Tahir M, Mohan A, Seith A. Radiological manifestations of splenic tuberculosis: a 23-patient case series from India. Indian J Med Res. 2007;125:669–78.
22. Pastakia B, Shawker TH, Thaler M, O'Leary T, Pizzo PA. Hepatosplenic candidiasis: wheels within wheels. Radiology. 1988;166:417–21.

23. Chou YH, Tiu CM, Chiou HJ, Hsu CC, Chiang JH, Yu C. Ultrasound-guided interventional procedures in splenic abscesses. Eur J Radiol. 1998;28:167–70.
24. Warshauer DM, Hall HL. Solitary splenic lesions. Semin Ultrasound CT MR. 2006;27:370–88.
25. WHO Informal Working Group. International classification of ultrasound images in cystic echinococcosis for application in clinical and field epidemiological settings. Acta Trop. 2003;85:253–61.
26. Goerg C, Schwerk WB, Goerg K. Sonography of focal lesions of the spleen. AJR Am J Roentgenol. 1991;156:949–53.
27. Goerg C, Schwerk WB, Goerg K. Splenic lesions: sonographic patterns, follow-up, differential diagnosis. Eur J Radiol. 1991;13:59–66.
28. Chiavaroli R, Grima P, Tundo P. Characterization of non-traumatic focal splenic lesions using contrast enhanced sonography. JCU. 2011;39; 310–315.
29. Gorg C, Weide R, Schwerk WB. Malignant splenic lymphoma: sonographic patterns, diagnosis and follow-up. Clin Radiol. 1997;52:535–40.
30. McKenney KL, Nuñez DB Jr, McKenney MG, Asher J, Zelnick K, Shipshak D. Sonography as the primary screening technique for blunt abdominal trauma: experience with 899 patients. AJR Am J Roentgenol. 1998;170:979–85.
31. Perret RS, Sloop GD, Borne JA. Common bile duct measurements in an elderly population. J Ultrasound Med. 2000;19:727–30.
32. Romano AJ, vanSonnenberg E, Casola G, Gosink BB, Withers CE, McCutchan JA, Leopold GR. Gallbladder and bile duct abnormalities in AIDS: sonographic findings in eight patients. AJR Am J Roentgenol. 1988;150:123–7.
33. Raghavendra BN, Subramanyam BR, Balthazer EJ, et al. Sonography of adenomyomatosis of the gallbladder: radiologic pathologic correlation. Radiology. 1983;146:747.
34. Sommer FG, Taylor KJ. Differentiation of acoustic shadowing due to calculi and gas collections. Radiology. 1980;135:399–403.
35. Andrén-Sandberg A. Diagnosis and management of gallbladder polyps. N Am J Med Sci. 2012;4:203–11.
36. Ralls PW, Halls J, Lapin SA, Quinn MF, Morris UL, Boswell W. Prospective evaluation of the sonographic Murphy sign in suspected acute cholecystitis. J Clin Ultrasound. 1982;10:113–5.
37. Marton KI, Doubilet P. How to image the gallbladder in suspected cholecystitis. Ann Intern Med. 1988;109:722–9.
38. Jeffrey RB Jr, Nino-Murcia M, Ralls PW, Jain KA, Davidson HC. Color Doppler sonography of the cystic artery: comparison of normal controls and patients with acute cholecystitis. J Ultrasound Med. 1995;14:33–6.
39. Bloom RA, Fisher A, Pode D, Asaf Y. Shifting intramural gas—a new ultrasound sign of emphysematous cholecystitis. J Clin Ultrasound. 1984;12:40–2.
40. Cornwell EE III, Rodriquez A, Mirvis SE, et al. Acute acalculous cholecystitis in critically injured patients. Preoperative diagnostic imaging. Ann Surg. 1989;210:52.
41. McGahan JP, Lindfors KK. Acute cholecystitis: diagnostic accuracy of percutaneous aspiration of the gallbladder. Radiology. 1988;167:669–71.
42. Haubek A, Pedersen JH, Burcharth F, Gammelgaard J, Hancke S, Willumsen L. Dynamic sonography in the evaluation of jaundice. AJR Am J Roentgenol. 1981;136:1071–4.
43. Dewbury KC, Joseph AE, Hayes S, Murray C. Ultrasound in the evaluation and diagnosis of jaundice. Br J Radiol. 1979;52:276–80.
44. Vallon AG, Lees WR, Cotton PB. Grey-scale ultrasonography in cholestatic jaundice. Gut. 1979;20:51–4.
45. Laing FC, Jeffrey RB Jr, Wing VW. Biliary dilatation: defining the level and cause by real-time ultrasound. Radiology. 1986;160:39.

46. Muhletaler CA, Gerlock AJ Jr, Fleischer AC, James AE Jr. Diagnosis of obstructive jaundice with nondilated bile ducts. AJR Am J Roentgenol. 1980;134:1149–52.
47. Freeman ME, Rose JL, Forsmark CE, Vauthey J. Mirizzi syndrome: a rare cause of obstructive jaundice. Dig Dis. 1999;17:44–8.